

POLITECNICO DI TORINO

Department of Mechanical and Aerospace Engineering
Class LM-33 (DM270)



**Politecnico
di Torino**

Master's Thesis in Automotive Engineering

Model-based vehicle dynamics control system and states estimation for 4WD Formula SAE electric vehicle.



SQUADRA | CORSE
POLITO

Tutors:
Prof. Andrea Tonoli
Eng. Raffaele Manca

Candidate:
Luca Massano

Academic Year 2022/2023

Dedicata a...

Contents

Contents	4
Abstract	6
1. Introduction	7
1.1. Formula Student	7
1.3. Squadra Corse PoliTO	10
1.4. SC22evo Overview	11
1.5. Vehicle Dynamics & Control Systems Department	13
1.6. Vehicle Dynamics Controllers	13
1.7. SC22 Vehicle Control System	16
1.8. Thesis Outline	19
2. State of the Art	20
2.1. Side Slip Angle Estimation	20
2.1.1. Kinematic Estimator	20
2.1.2. Observer-based Estimator	21
2.1.3. Neural Network-based Estimator	22
2.2. Yaw Controller for Electric Vehicle State of the Art	24
2.2.1. PID Controller	24
2.2.2. Integral Sliding Mode Controller	25
2.2.3. Fuzzy Logic Controller	27
2.2.4. Linear Quadratic Regulator	28
2.2.5. Feed Forward	28
2.2.6. Model Predictive Control	29
3. Methodology	31
3.1. State Estimation	31
3.1.1. Vehicle States Estimation	31
3.2. Yaw Control	37
3.2.1. A-LQR	37
3.2.2. Model-Based Feed Forward	38
3.3. Motor Torque Allocation	40
4. Numerical Results	42
4.1. Vi-CarRealTime	42
4.2. Key Performance Indicators (KPIs) Definitions	43
4.3. Standard Manoeuvres	44
4.3.1. Constant Radius Cornering	44
4.3.2. Ramp Steer	48

4.3.3.Sine Sweep Steer	51
4.4. Max Performance Events	55
4.4.1.State Estimation	56
4.4.2.Yaw Control	59
4.4.3.Motor Torque Allocation	61
5. Experimental Validation	62
5.1. Hardware Deployment	62
5.2. Sideslip Angle Estimation Validation	63
6. Conclusions and future works	66
References	67
List of Figures	69
List of Tables	71

Abstract

Yaw Control is a common topic on high performance race cars vehicle dynamics. Compared to Yaw Control for passenger cars, the application to high-performance vehicles is mainly focused on improving drivability, reactivity and performance through the partial or total achievement of a desired cornering behaviour, obtained through vehicle states tracking.

The subject of this analysis is the development of a Yaw Control for the Formula Student (FS) 4-Wheel-Drive (4WD) electric race car of Squadra Corse PoliTo. The prototype is equipped with four electric motors, independently controlled, driving one wheel each, guaranteeing high flexibility in torque control. Thus, in this application, Yaw Control is obtained exploiting Torque Vectoring (TV) strategy, so obtaining a torque unbalance between left and right wheels during cornering, to help the vehicle behave in the desired way.

The desired cornering vehicle behaviour is decided generating reference signals for Yaw Rate and Side Slip Angle, two fundamental states for lateral vehicle dynamics. Yaw Rate reference is compared to measured Yaw Rate, while Side Slip Angle reference is compared to an estimated Side Slip Angle, since measuring that state is not suitable for the application, apart from using very expensive sensors. For this reason, an EKF-based combined with a kinematic-based Side Slip Angle estimator has been decided to be implemented, to have a reliable state estimation.

This work aims to propose, adapt, and implement a solution to improve vehicle performance during transient and steady state manoeuvres, through the adoption of a combination of a LQR and model-based Feed Forward TV Yaw Control strategy. This solution has been decided to be used, considering actual state of the art Yaw Control strategies, considering ease of implementation, accuracy and computational effort to run in an ECU.

Both the state estimator and the control logic are implemented and tested in a Matlab/Simulink and Vi-CarRealTime co-simulation environment. The goodness of the results are showed analysing cost function trends, typical performance-related vehicle signals and lap-time on Formula Student Skidpad Event. Comparative analysis are carried out between controlled and uncontrolled vehicles, both on standard automotive manoeuvres like constant radius cornering, ramp steer and sine sweep steer, and on real FS event. Moreover, the controller, together with the state estimator, has been deployed on the Squadra Corse PoliTo prototype's ECU (dSpace MicroAutobox II) for track testing and validation: the Sideslip Angle estimator has been validated using a Kistler Ground Speed Sensor.

Results show a reduction of Skidpad simulation lap-time of 5% and RMS error between estimated and measured Side Slip Angle of 0.0172 rad.

1. Introduction

The design of a race car is mainly focused on the achievement of target performances of the vehicle. Generally, everything is a trade-off between low cost, light weight and reliability. Today, the number of electronically controlled devices and actuators is increasing, opening the possibility to a new way to improve vehicle performances: control strategies. Being just strategies and algorithms, controls can exploit already existing actuators to improve vehicle performances, without any additional costs or weight.

The subject of this work is the analysis of the performances that a new controller, a Yaw Controller, can bring to a fully electric race car. The vehicle under investigation is the Formula Student vehicle of the Politecnico di Torino racing team, Squadra Corse PoliTo. With a 4-independent-motors powertrain, the vehicle controllability is the core of the design, being one of the most important reason to chose such architecture, rather than a lighter and cheaper 2WD solution.

1.1. Formula Student

Formula Student is an engineering competition in which more than 200 University teams from more than 60 countries challenge on a multidisciplinary basis.

The competition is subdivided into three main categories: Combustion Vehicles, Electric Vehicles and Driverless Vehicles (combustion or electric is not giving any difference).

Squadra Corse PoliTo competes in Electric Vehicle class, which has become the most diffused and competitive in the last years.

As mentioned above, the competition is an engineering challenge, and not a racing championship: this means that for succeeding in Formula Student events, the team must be excellent in all engineering disciplines. Due to this, a typical Formula Student competition is subdivided into Static Events and Dynamic Events.

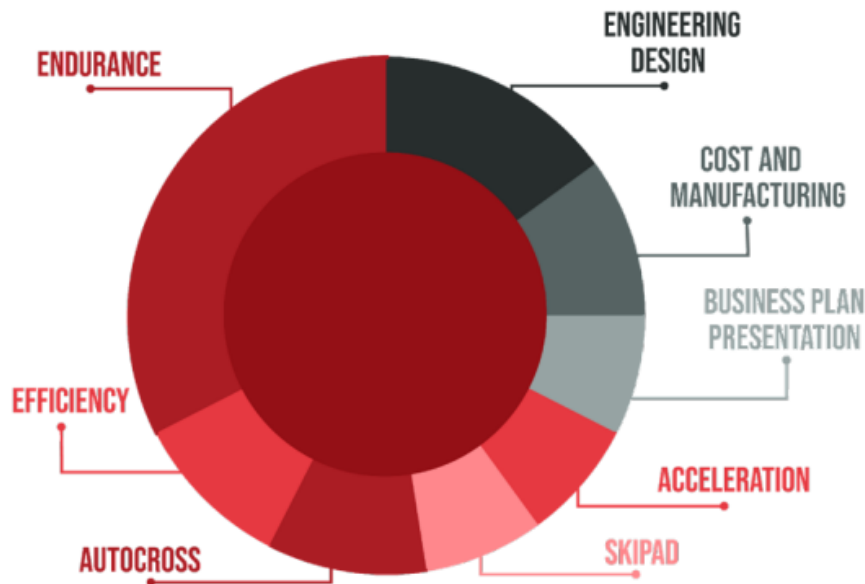


Figure 1: Formula Student Events

Static Events are three: Engineering Design, Business Plan Presentation and Cost and Manufacturing.

The Engineering Design consists of presenting all the engineering choices performed by the team during the design phase of the season so to obtain the manufactured vehicle. Each choice must be clearly explained and justified to a group of expert judges coming from different automotive companies and belonging to different engineering areas.

The Cost and Manufacturing has the target of explaining and justifying the team's costs of the current season, with a focus on the environmental impact of the production of a particular vehicle subsystem.

Business Plan Presentation consists in a simulating a real business plan case study. The target is to find the best innovative business idea to sell the car or everything related to it. An entire financial analysis is needed, from the idea, to the product one, passing from market forecast, marketing and future trends. Everything has to be presented to a team of judges that will act as potential business investors and will decide whether the idea is innovative and the business study has been well conducted.

The dynamic events, instead, directly involve the competing vehicle, even if in the Formula Student Germany regulation (the official competition rulebook) is clearly stated that any wheel to wheel racing is prohibited. Any point scored by the team in each Dynamic Event is only depending on the relative difference between the team and the best team on that event (or, for the Efficiency event, the relative difference between the consumed energy compared to the best team).

The Dynamic events are four: Acceleration, Skidpad, Autocross and Endurance.

The Acceleration Event consists of an acceleration from standing still of 75 meters long track, three meters wide.

The Skidpad event consists of an eight-shaped track with a width of three meters. The two circles drawing the eight shape have a central radius of 9.125 meters. The driver must complete the two right circles and then the two left circles. Only the

second run for each side is timed and the final lap-time is the average of the two second run.

The Autocross Event is a single lap starting from standing still. The track can be open or closed circuit, generally with a total length of approximately one kilometre, with a minimum track width of three meters. There are other characteristics such as the maximum straights length or minimum hairpins radius.

Finally, the Endurance Event is the most important event. It consists of a long run race of 22 kilometres, divided into two stints of 11 kilometres each. A driver change is mandatory at the end of the first stint. In this event, vehicle performances are not the key for the victory: tire and energy management, as well as vehicle overall reliability are the most important factors to succeed.

1.3. Squadra Corse PoliTO

Squadra Corse PoliTO is the Formula Student team of the Politecnico di Torino. Born in 2004 with the target of competing in the Formula student championship, the first vehicle was ready in 2005, racing that summer in the Combustion category.



Figure 2: SC05 (Squadra Corse PoliTo 2005 prototype)

The Internal Combustion Engine prototype development proceeded until 2009, when the first hybrid prototype was designed starting from 2008 prototype. It raced during summer 2010 events, winning the world championship.



Figure 3: SC08H (Squadra Corse PoliTo 2010 prototype)

The first Electric prototype arrived in 2012, when Squadra Corse PoliTO became the first Italian team to participate to Formula Student Electric category. From that year up to now, the vehicle has always remained fully electric, pushing the research and development with the target of reducing weight, improving aerodynamic efficiency and improving control strategies.



Figure 4: SC12e (Squadra Corse PoliTo 2012 prototype)

During the 2022 season the team participated to three events: FSATA (Formula SAE Italy), FSG (Formula Student Germany) and FSAA (Formula Student Alpe Adria, Croatia).

The team scored three silver medals at FSATA and one bronze medal at FSAA, but due to electrical related reliability problems, the team was not able to be competitive for the entire competition.

The vehicle finished the Acceleration event in 3.56 seconds, the team overall record.

The 2023 season is mainly focused on increasing the overall system robustness and reliability. The team is composed by 65 students coming from 10 different engineering courses working together to optimize the 2022 vehicle and compete with a fully reliable vehicle in summer 2024.

The team is organized in different departments, working independently, but cooperating to achieve a common goal:

- **Aerodynamics & CFD:** they are responsible of designing, manufacturing and validating in the wind tunnel all the aerodynamic package of the vehicle. Moreover they perform all CFD analysis of other divisions
- **Battery Pack:** they are responsible of designing and assembling the low voltage and high voltage batteries of the vehicle.
- **Chassis & Composites:** they are responsible of designing and manufacturing the vehicle chassis and the impact attenuator. Moreover they are responsible of all studies on composite materials of the vehicle.
- **Communication & Media:** they are responsible of every social media, content creation and event of the team.
- **Electronics:** they are responsible of designing and manufacturing all the electronic components present on-board.
- **Management:** they are responsible of managing the cash flow of the team, as well as making strong relationships with suppliers and managing all the Static Events.
- **Powertrain:** they are responsible of managing, testing and calibrating inverters and motors
- **Thermal Management:** they are responsible of designing and manufacturing all the cooling system of the vehicle (battery, inverters, motors)
- **Unsprung Masses & Geartrain:** they are responsible of designing and manufacturing all the unsprung masses of the vehicle (rim, suspensions, transmission, uprights, braking system) and the steering assembly.
- **Vehicle Dynamics & Control Systems:** they are responsible of the early season target setting, every full vehicle simulation, suspension kinematics, telemetry, data analysis and the complete control system. Moreover, they are responsible of track tests and driver trainings.

1.4. SC22evo Overview

The 2023 Squadra Corse PoliTO prototype is, by regulations constraints, a single-seater open-wheel formula-like car.



Figure 5: SC22evo (Squadra Corse PoliTo 2023 prototype)

Vehicle main data	
Mass without driver	211 kg
Front mass repartition	47.5 %
Wheelbase length	1.525 m
Front and rear tracks width	1.202 m
Center of Gravity height from ground	0.28 m
Tires	185/40 R13 slick
Rims	R13 magnesium-aluminum alloy
Aerodynamic Lift coefficient	4.78
Aerodynamic Drag coefficient	1.48
Nominal HV battery pack capacity	7.7 kWh
Nominal HV battery pack voltage	574.2 V

Table 1: SC22evo prototype main data

The vehicle chassis is characterized by a CFRP and aluminum honeycomb sandwich monocoque, aluminum and steel anti-rollover tubes and aluminum honeycomb impact attenuator.

Vehicle suspensions are double wishbone with fully adjustable pushrod layout made of CFRP tubes, connected by uniball joints to the monocoque and to the machined aluminum uprights.

The powertrain, as stated before, is fully electric coming from AMK Formula Student racing kit. It includes four IGBT inverters and four SPM-IPM Electric Motors, each one independently controlled by a single inverter. Each motor guarantees a maximum torque of 21 Nm and maximum velocity of 20000 rpm, reaching up to 35 kW of maximum power. The powertrain is so able to develop 140 kW at 600 V DC, but the power is limited by FSG regulations at 80 kW at the DC battery output bus. Motors are in-wheel, outboard-mounted, transferring power to tires through a double-stage planetary transmission with a single gear ratio of 14.69:1.

The High Voltage battery pack is made of two parallels of 132 series of pouch Li-Po cells. The battery pack has a nominal capacity of 7.7 kWh at nominal voltage.

The on-board signals run through four CANs that are managed by the dSpace MicroAutobox II Electric Control Unit, through the Vehicle Control System installed in it.

1.5. Vehicle Dynamics & Control Systems Department

Vehicle Dynamics and Control System department is one of the departments of Squadra Corse PoliTo team. It is divided into two smaller teams that cooperate with the target of improving overall drivability and performance on track.

Vehicle Dynamics

The responsibilities of the Vehicle Dynamics team during the season are

- Target setting for the upcoming vehicle, based on data analysis of previous dedicated track tests: mass, aerodynamic parameters, stiffness and damping distribution, chassis torsional stiffness, HV battery energy, maximum accelerations achievable for static mechanical component design.
- Tire performance study to give indications on how performances change due to load, pressure, and suspension characteristic angles.
- Suspension kinematics design to optimize dynamic toe and camber angles during motion to let the tire work under best conditions.
- Track tests organization, management and data analysis to fine tune vehicle setup and control system tuning parameters to validate the design and optimize performances.

Control System

The responsibilities of the Control System team during the season are

- Full vehicle simulations using ViGrade Vi-CarRealTime software in co-simulation with Matlab/Simulink environment, updating vehicle static parameters as the season proceed.
- Developing, testing, and validating new control strategies or upgrading previous ones.
- Managing and fine-tuning the developed control system on track, through C-code compilation and flashing into dSpace MicroAutobox II Electric Control Unit.

1.6. Vehicle Dynamics Controllers

Integrated Chassis Control (ICC) is one of the cores of current research on vehicle dynamics applied control systems thanks to the possibility of having a continuously increasing number of on-board chassis actuators. ICC main target is safety, comfort and performance improvement.

Electric motors are driving the development of first generation of ICC, thanks to their applicability and scalability (from simple low-voltage hybrid passenger cars to high voltage full electric hyper cars) and their ease of control: since the torque of an electric motor is directly proportional to the torque current passing through it, its torque demand becomes a simple current demand to the inverters.

ICC can be classified with two principal categories: Downstream Architecture and Upstream Architectures (Mazzilli V., 2021).

The first architecture refers to a horizontal structure of the complete control system, in which the control systems work independently until being coordinated at the

actuators stage (i.e. the lowest level of the architecture). This architecture guarantees high recovery possibilities, since every controller is independent from each other, the malfunctioning of a control strategy does not prevent the correct working of the others.

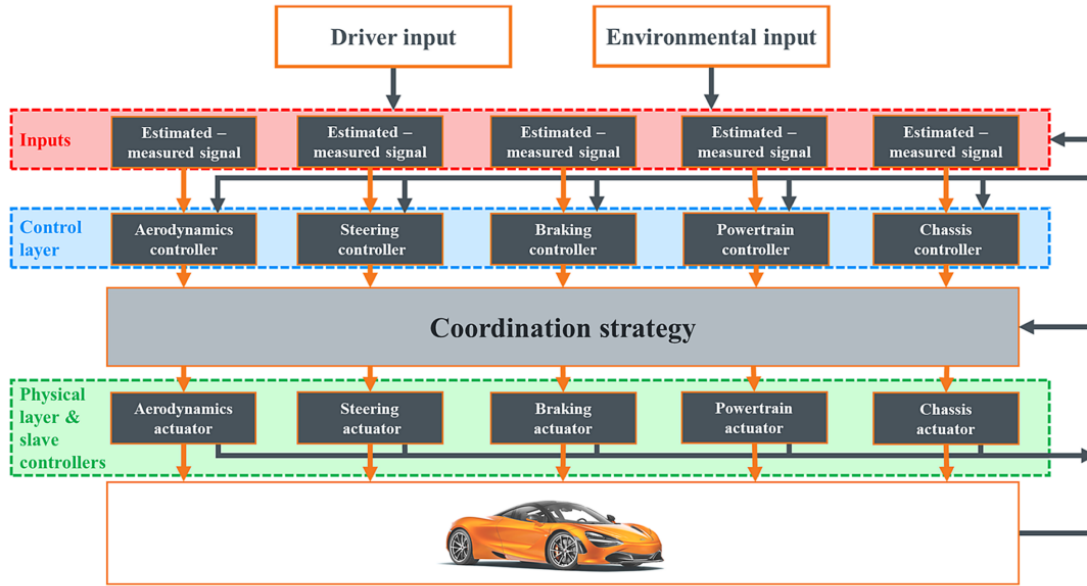


Figure 6: Downstream ICC Architecture Example (Mazzilli V., 2021)

The second category, instead, refers to top-down architectures, in which high level multivariable controllers are placed between sensors (or states estimation) and actuators (Mazzilli V., 2021). An example of this architecture can be the multi-level coordination in which the controller's coordination and monitoring is subdivided in a control slack as follows:

1. Supervision Strategy: it selects the control mode and computes the references for signals, depending on the considered states.
2. High-level Controller: it computes the control actuations to track the previously computed reference(s).
3. Coordination Strategy: it selects the control logic depending on what the Supervision Strategy decided the previous time instant.
4. Control Action Strategy: it distributes the control actuation signals to the actuators.
5. Individual Actuator Control: it defines the final low level control action to each selected actuator.
6. Physical Layer: the actuators perform, when possible, the actuation decided at the IAC layer and modifies the vehicle dynamics.

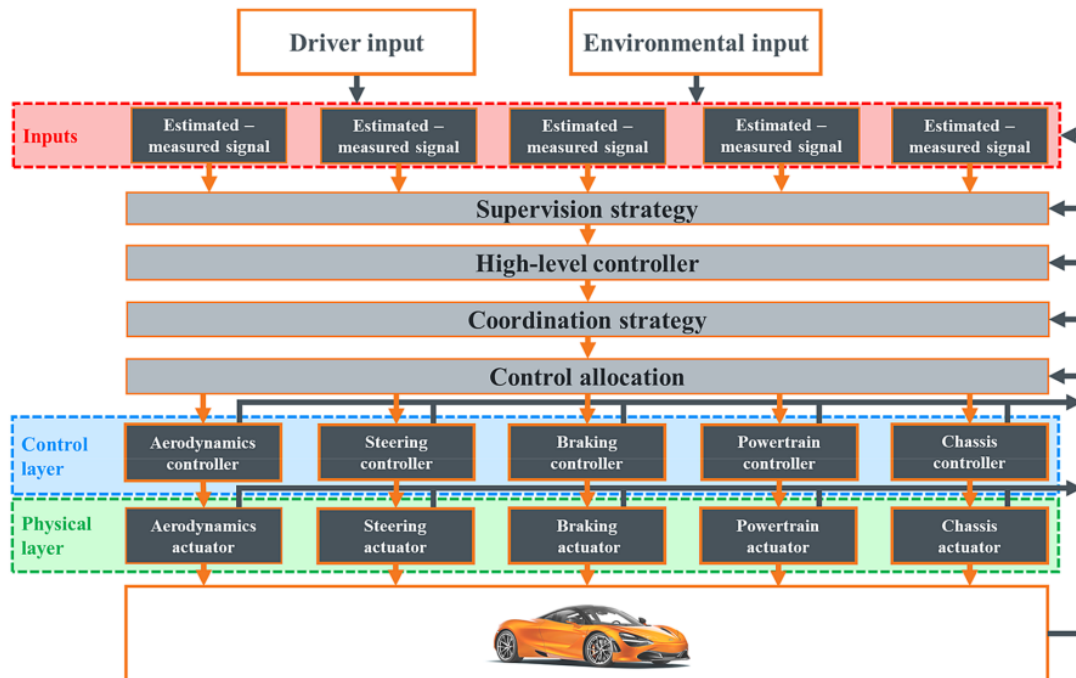


Figure 7: Upstream ICC Architecture (Mazzilli V., 2021)

The Control System that will be analyzed in this work is more similar to a Downstream Approach, since the on-board control system is a cascade of smaller controllers. Here it follows a summary of the most diffused ICC strategies.

Attitude Control

Attitude Control consists of controlling the vehicle body motions (roll, heave, pitch) in order to minimize them with the target of improving the ride comfort and performance. It includes Active Suspension systems, Continuous Damping Control and Active Roll Control. Active and semi-active suspensions are the most used actuators for the Attitude Controllers, as well as active torsion bars since they can actively control roll, heave and pitch stiffnesses and damping to achieve the desired body motion.

Slip Control

Slip Control consists of controlling the tire longitudinal slip of the driving wheels. This is needed in order to overcome the optimal tire longitudinal slip guaranteeing the best ratio between longitudinal and vertical force at the tire contact patch.

The two main categories of Slip Controllers are Traction Control Systems and Antilock Braking Systems: the first controls the wheel motion during traction, acting on what brings traction to the driving wheels, while the second controls the wheel motion during braking, acting on the vehicle braking system.

It is clear how maximizing the tire performances, letting it work around the optimal slip region can be very challenging and a lot of information regarding tire properties are needed. Moreover, the road condition, such as dry, wet, snow, ice, must be known a-priori to know the maximum exploitable friction coefficient for the vehicle longitudinal motion.

Yaw Control

This category of controllers is fundamental to improve vehicle lateral dynamics, generally exploiting vehicle Yaw Rate and Side Slip Angle tracking to improve performances and stability at the same time. Also in this case, Yaw Controllers are divided into two categories: Torque Vectoring and Electronic Stability Control.

The Torque Vectoring generally applies positive torques on the driving wheels. The torque distribution is performed generating a torque unbalance between left and right side of the vehicle, generating a resultant Yaw Moment that helps the vehicle behaving in the desired controller way, that can be understeering, neutral or oversteering. With passenger cars, it is generally desired a slightly understeering behavior since the vehicle is more stable and easier to drive and control. With sports car, instead, the target is to tune the desired behavior according to the driver needs or letting the vehicle behave as neutral as possible to increase the driver freedom to operate.

Being the actuation a positive torque unbalance, it is limited to vehicles with independently controllable motors or electronically actuated differential: for this reason, it is not very diffused on current road vehicles, but it's likely to grow soon with the market increase of electric vehicles. For sports cars, instead, it is way more diffused.

Electronically Stability Control, instead of generating a positive torque unbalance between left and right side of the vehicle, acts on the braking system to generate a negative torque unbalance. Acting on the braking system, it is possible to implement this control strategy on the majority of current road vehicles, with the target of improving stability and drivability, with the possibility of degrading the longitudinal dynamics applying negative torque (i.e. decelerating) the vehicle.

1.7. SC22 Vehicle Control System

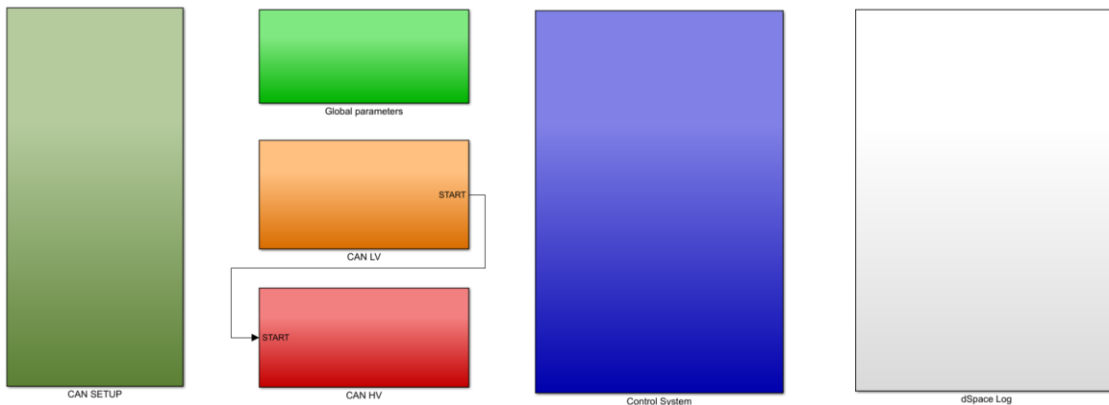


Figure 8: Simulink high-level model of SC22 Vehicle Control System

The complete Vehicle Control System is the responsible for the managing of all signals and information coming from the four CAN. As can be seen from Figure 8, it is divided into six parts:

- CAN SETUP: in this block, all the Rx/Tx CAN communications are performed.
- Global Parameters: in this block, all vehicle physical parameters, as well as control system tuning parameters are set.

- CAN LV: in this block, sensor acquisitions and electronic boards compliant with Formula Student rules dialogue. For example, the Ready-to-Drive procedure to switch on the vehicle is managed here.
- CAN HV: this block is dedicated to the High Voltage Battery Management System and to handle any possible error or problem coming from HV system.
- Control System: this block is the Vehicle Dynamics-related control system part. It contains all the strategies to control vehicle behavior during motion.
- dSpace Log: in this block, only data logging is performed.

The complete Vehicle Control System is developed in Matlab/Simulink environment, and it is compiled in C programming language, with dSpace proprietary compiler to be easily run on the ECU.

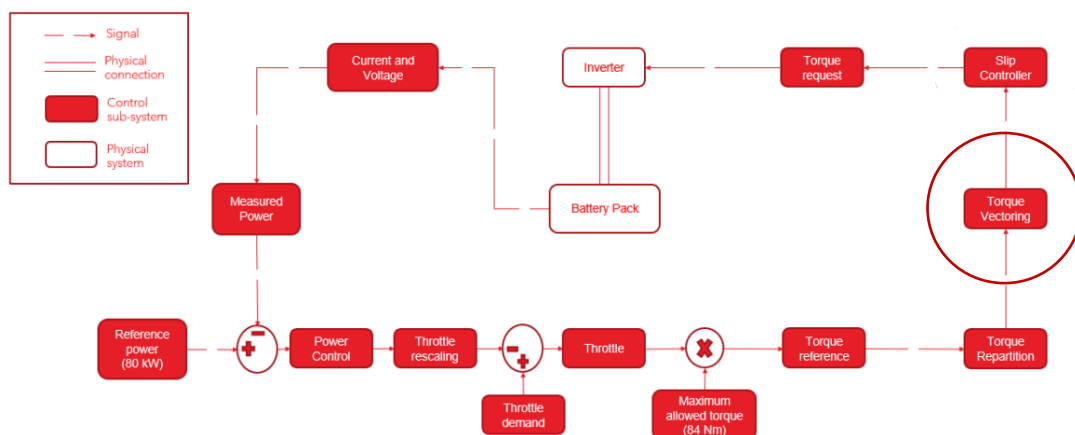


Figure 9: Control System Structure with a focus on what will be developed in this work.

The Control System most important target is to generate the torque request to be sent as input to the four inverters, starting just from driver actuations on accelerator and braking pedals and on steering wheel. The driver demand during motion is called “Throttle demand”, representing the percentage (positive during traction, negative during braking) of accelerator or braking pedals request. Throttle demand can be scaled, when necessary, by the Power Control.

The Power Control is a PI controller that controls electric power not exceeding 80 kW as imposed by Formula Student regulation (The limit must not be exceeded by the power signal after a sliding-window moving average filter of 500 ms is applied on it). The reference is a constant power of 80 kW, while the actual electric power is computed multiplying DC Bus Current and DC Bus Voltage. When there is positive error (so the actual power overcomes the imposed reference), the Power Control acts as throttle rescaling: a positive amount that will be subtracted to the actual throttle demand. Torque reference is then generated as the corrected Throttle multiplied by the maximum allowed torque (84 Nm in the best scenario).

Then, the total torque request is distributed to the front and rear axles through a static torque repartition during traction, with the optimal traction condition achieved at 30% torque to the front wheels, or a dynamic torque repartition during

regenerative braking, always guaranteeing the requested overall braking balance, considering the dynamic growth of the mechanical braking torque.

After that, and, by now, only during traction manoeuvres, the Torque Vectoring (TV) controls the eventual left/right motor torque unbalance to guarantee state tracking. State estimation, tracking and TV are the main focuses of this work and later will be explained more in deep.

Finally, the Slip Controller will control each wheel independently with the target of reducing the tire longitudinal slip when it overcomes a pre-defined threshold. It works both in traction and braking condition and the target is to reduce the absolute value of the applied torque whenever tire slippage occurs.

After the Slip Controller, the torque request is sent to the Inverter Control Board (after all the checks regarding HV Battery, Inverters and Motors overtemperature constraints and eventual field weakening region) that will translate the torque request in a physical current action in the motors that will generate the desired torque and they are the responsible of the speed control of the motors.

Motors Speed Control

The motors speed control is simpler to implement compared to the torque control, since once the imposed speed target is achieved, inverters automatically control motor torques to guarantee the desired speed. It is important to underline that the Control System imposes a torque request to inverters and not a speed request. Inverters require three inputs for the motor control:

- Target Velocity: constant positive value during traction or constant zero value during coasting and braking.
- Minimum Torque: maximum (as absolute value) torque that can be achieved during regenerative braking, and it's kept constant.
- Maximum Torque: it's the output of the Control System, and it's used as torque request during motion.

When motors are at a different speed compared to the Target Velocity, inverters will command to each motor the torque requests coming from the Control System that will guarantee traction or braking depending on the driver request. With this control strategy, the required torque can always be applied, except for being at the target velocity. In this way, the motor torques can be dependent on driver inputs, guaranteeing drivability, predictability, and controllability. This behavior can be demonstrated logging a feedback signal coming from the motor: the excitation current. AMK, the powertrain manufacturer, also gives an indication on the relation between excitation current and applied torque: there is a direct proportionality with a gain equal to 0.26 called motor torque constant.

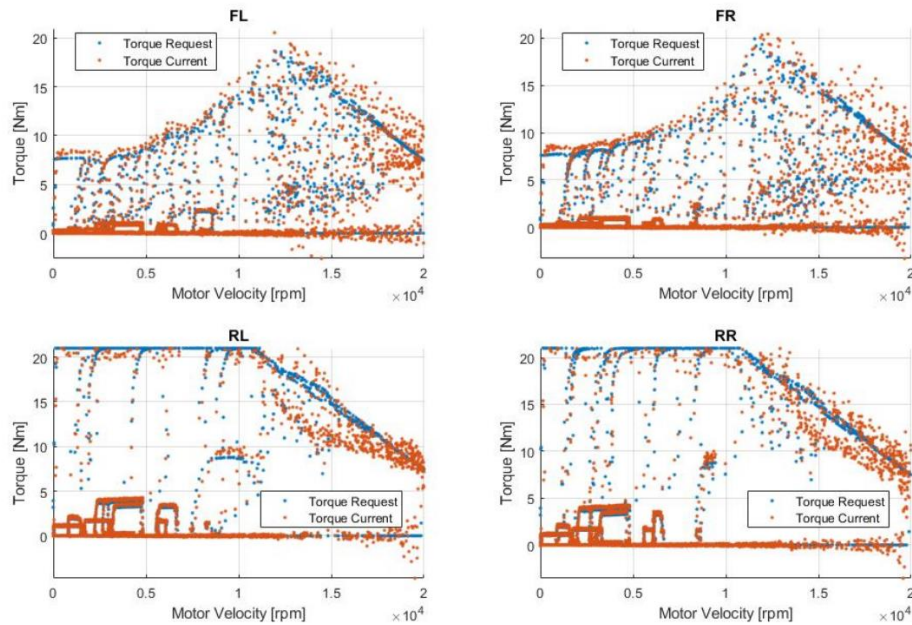


Figure 10: Motors Speed Control

Figure 10 represents, on the same plot, the requested torque coming from Control System module in blue and the actual motor delivered torque in orange as function of each motor speed during a track lap. Trends are very similar between Requested torque and Delivered torque, meaning that motors control is working well.

Low rpm, high torque region is not populated for the two front motors, due to Traction Control torque scaling during high traction requests at low speed, in which the vehicle has low grip due to low downforce and the front axle loses load due to load transfer to the rear.

1.8. Thesis Outline

This work is structured as follows:

- Chapter 2 presents the state of the art for vehicle State Estimation and Yaw Control Systems
- Chapter 3 presents the chosen and applied methodologies for vehicle State Estimation and Yaw Control Systems
- Chapter 4 presents the obtained results in co-simulation.
- Chapter 5 presents the validation of the work.

2. State of the Art

To develop a complex control strategy like the Yaw Control, it is important to analyze what strategies are already existing, what are the most diffused and which technique can best suit our application, considering accuracy, responsiveness, and computational effort.

But before, an overview of current techniques of state estimation is needed, since a proper Yaw Control works exploiting Yaw Rate and Side Slip Angle as feedback signals. Yaw Rate, in our application, is measured through a 6-axis Inertial Measurement Unit (IMU), while Vehicle Side Slip Angle is not. The reason behind this choice is the complexity and the cost of currently available sensors directly measuring that state, for example optical sensors or high-precision two-points GPS systems. For this reason, Side Slip Angle must be estimated and a literature review is necessary.

2.1. Side Slip Angle Estimation

Side Slip Angle is defined as the angle between vehicle's longitudinal axis and the direction of travel (direction of the velocity vector), taking direction of travel as reference (Chindamo, 2018). Its estimation is necessary for every vehicle with a lateral dynamics-oriented control system, since its tracking guarantees vehicle stability. Its first online estimation is dated to early 1990s with the introduction of the first Electronic Stability Control (ESC) on passenger cars (Chindamo, 2018).

The target of side Slip Angle estimation and, consequently, tracking the desired value, is to avoid such state to become large enough to lose drivability and achieve instability.

In literature, three methods are used to estimate Vehicle Side Slip Angle:

- Kinematic Approach
- Observer-based estimation
- Neural Network-based estimation

2.1.1. Kinematic Estimator

From literature, it's well known that side slip angle is not directly computable using common signals running on-board on vehicle CAN.

On the other hand, it's well known how to compute its derivative (rajamani, 2009), that is, instead, just depending on vehicle signals like lateral acceleration, longitudinal velocity and yaw rate.

$$\dot{\beta}_{kin} = \frac{a_{Y,Ch}}{V_x} - r + g \sin \phi_r$$

Φ_r is the value in radians of the road banking, so the angle formed by the road with respect to the horizontal, in ZY plane. For our application, this quantity can be assumed to be always zero without losing any estimation precision.

In a deterministic, continuous time, system, integrating this derivative knowing the initial value of the state, would give a perfect Side slip Angle estimation. In real systems, all signals involved in this estimation are not noise-free and the relative noise does not cancel out after math operations.

Noise is generally seen as a gaussian distribution with a certain mean and variance (Welch, 2006). For real applications, the noise mean value cannot be assumed to perfectly zero. This means that, integrating the Side Slip Angle derivative would always tend to state divergence, accumulating noise error during integration. For this reason, kinematic estimator alone cannot be implemented for real-time state estimation. In literature, it can be found that kinematic estimators can be anyway used in parallel to observer-based estimators to improve the latter precision, transient responsiveness and speed of convergence.

2.1.2. Observer-based Estimator

This approach estimates Side Slip Angle starting from a selected vehicle model, available vehicle on-board signals and vehicle physical and geometrical parameters. Due to the need of a physical model, the estimation accuracy will be strictly related to the complexity of the model, the accuracy of signals and the precision of vehicle parameters.

In literature, observers used for this application are Luemberg Observer (LO), Sliding-mode Observer (SMO) and Kalman Filter (KF), with this one the most used, with a total of 71 publications out of 120, in the area of observer-based Side Slip Angle estimation (Chindamo, 2018).

LO is a simple observer and is rarely used. SMO is slightly more complicated than LO, but anyway they are only working for deterministic systems, meaning that a perfect knowledge of the vehicle model is needed and input signals must be completely without noise. This is clearly a big limit for online, real-time estimation.

KF, instead, can work properly even with some small model uncertainty and signal noise, maintaining a relative simplicity of implementation. Due to this important feature, KF (and its variants) is the most used observer-based estimator, thanks to its robustness and stability.

For this reason, a deeper investigation for KF-based estimators is carried out.

Kalman Filter

Kalman Filter and its own variants (Extended Kalman Filter and Unscented Kalman Filter), addresses the general problem of estimating the state vector “x” of a discrete time, controlled process governed by these formulae:

$$\begin{aligned} \mathbf{x}_k &= f(\mathbf{x}_{k-1}, \mathbf{u}_{k-1}, \mathbf{w}_{k-1}) \\ \mathbf{z}_k &= h(\mathbf{x}_k, \mathbf{v}_k) \end{aligned}$$

With

- “f” being the system set of physical equations relating the actual state to the previous state, input and noise.
- “zk” is the system output (measured variables) and it’s related to the system states and noise through the set of equations “h”.
- “u” is the input vector.
- “w” and “v” are the process and measurement noises (Welch, An Introduction to the Kalman Filter, 2006).

Clearly, state vector “ x ” can be directly measured using first equation or inversely estimated using the second equation. The two methods will cumulate process error if used alone, because the first one (i.e., the dynamic system evolution) will be affected by uncertainty in the model parameters, while the second one (i.e., the measurement equation) will be affected by uncertainty in the measurement signals. These two uncertainties are represented by two matrices, Q and R , called covariance matrices. Kalman Filter (or its variants) simply generate the state estimation computing a weighted average between the two estimation strategies, based on Q and R values (Welch, An Introduction to the Kalman Filter, 2006).

Common KF-based estimation strategies for Side Slip Angle estimation use lateral vehicle models in which Side Slip Angle is a state, to perform the estimation. The most common vehicle models used for this kind of estimation are:

- Single track model
- Dual track model
- 7-DOF lateral dynamics vehicle model

Increasing the complexity of the model, together with increasing the model nonlinearities (tire characteristics, aerodynamics, ...), will increase an accuracy drop for the Kalman Filter due to its linear estimation properties. Nonlinearities can be better handled in the Extended KF that can manage nonlinearities through a model linearization about the state equilibrium point in which the model is at every time instant.

2.1.3. Neural Network-based Estimator

The Neural Network-based estimation technique, instead, is a data-driven approach, the opposite of the model-based approach, and it’s becoming more and more common for automotive applications (Genetic Algorithms, Neural Networks, Fuzzy Logics) (Chindamo, 2018).

Neural Networks are used for this application mainly because no vehicle model is needed: all the highly non-linear tire models, causing non-linear vehicle lateral dynamics, are totally substituted by the network.

The potentiality of Neural Networks is to find very good correlations between input signals and desired output(s) like, for this case, Side Slip Angle, just using math operations.

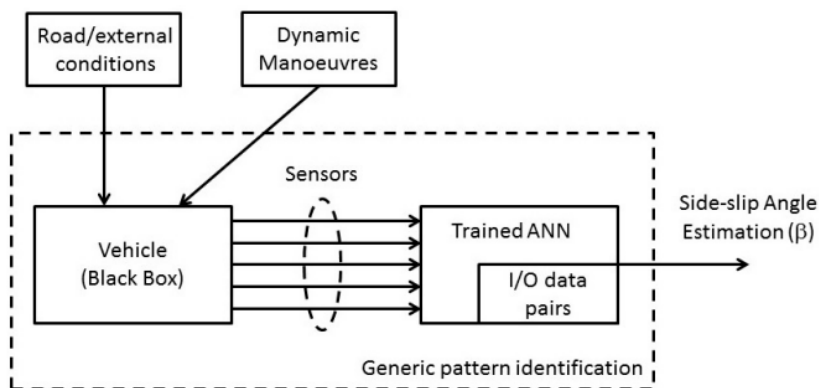


Figure 11: Artificial Neural Network (ANN) estimation process high-level schematic (Chindamo, 2018)

In literature, for this application, the chosen Neural Network has generally three layers: one input layer, one hidden layer, one output layer.

Input layer collects all lateral dynamics related signals like vehicle speed, steering angle, lateral acceleration and yaw rate, that are easily measurable on-board.

Hidden layer performs input combinations using nonlinear math operation (like sigmoid, logarithms, arctangents, ...), generating a layer rich of useful information, without any physical meaning.

Output layer combines hidden layer signals in a linear way (gains and offsets) to obtain a precise estimation of the vehicle Side Slip Angle.

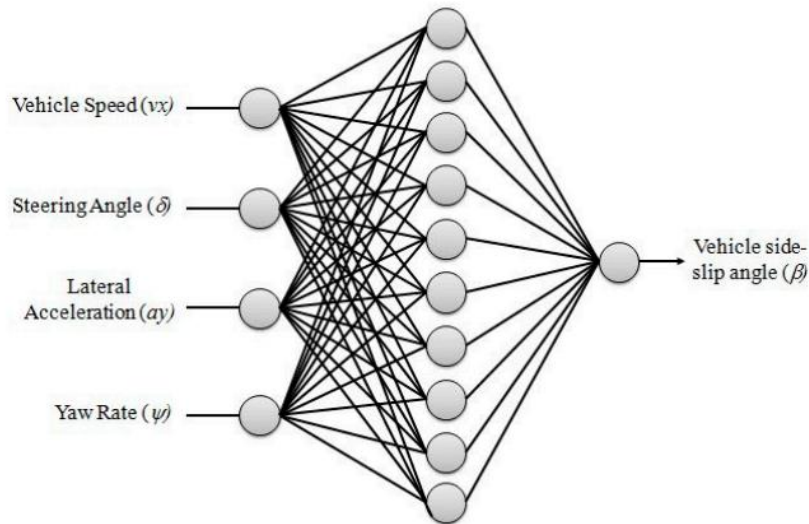


Figure 12: General layout of an ANN used for Side Slip Angle estimation (Chindamo, 2018)

The negative aspect of this application is that a lot of parameters must be chosen and tuned in order to have a precise estimation. This process of tuning is called ANN training and it's possible if and only if a lot of data logs are available, both for inputs and for outputs.

This means that the vehicle must run an offline test session equipped with some Side Slip Angle sensor, acquiring all needed data. Then, the ANN can be trained through back-propagation algorithm, trying to collect the set of parameters, gains and biases that will minimize the RMS error between measured and estimated Vehicle Side Slip angle on all the datasets.

Clearly, this negative aspect of running an offline session of testing with a complex, highly expensive sensor, together with the high online computational effort required by the ANN to estimate the Side Slip Angle in real time, makes this solution less suitable than observer-based side slip angle estimation.

For the reasons listed above, the estimation strategy in this work will be carried out mixing the steady state properties of an EKF together with transient properties of a kinematic-based approach.

2.2. Yaw Controller for Electric Vehicle State of the Art

The possibility of having a proper integrated full control algorithm is mainly thanks to the type of powertrain adopted by the SC22evo. In fact, four in-wheel motors can be controlled independently from each other, increasing the degrees of freedom the control can have. Compared to a standard internal combustion engine (ICE), an electric vehicle with this powertrain, can rely on a proper slip control during braking/traction together with a proper yaw control during cornering. This because at any time instant, each motor can do what required from the control logic.

From a controller point of view, the controlled variable is generally the Yaw Rate, since is easy to measure with sufficient accuracy in standard IMU for Formula SAE (SC22evo is equipped with a 6-axis IMU from SBG, measuring at same time accelerations in x, y, z directions and yaw, roll, pitch velocities).

In this chapter, several Yaw Control strategies are analyzed, representing the actual state of the art for BEV control strategies.

2.2.1. PID Controller

The Proportional-Integrative-Derivative (PID) is the most diffused controller. It is simple, reliable, easy to tune and very cheap from a computational effort point of view. The output of the controller (Action) is the sum of three, independent, actions.

- Proportional: it gives an action contribute proportional to the input (reference error) of the controller. It can reduce steady-state error and rise time but paying and increase in the overshoot.
- Integrative: it gives an action contribute proportional to the integral of the reference error. It's useful to eliminate completely the steady-state error.
- Derivative: it gives an action contribute proportional to the derivative of the reference error. Its effect is like a damping effect on the output, reducing overshoot and oscillations around the nominal value.

The complete formulation of this linear controller is the following, where $e(t)$ is the reference error, that for a Yaw Controller can be the Yaw Rate error or both Yaw Rate error and Side Slip Angle error.

$$C(t) = -K_p e(t) - K_i \int e(t) dt - K_d \frac{de(t)}{dt}$$

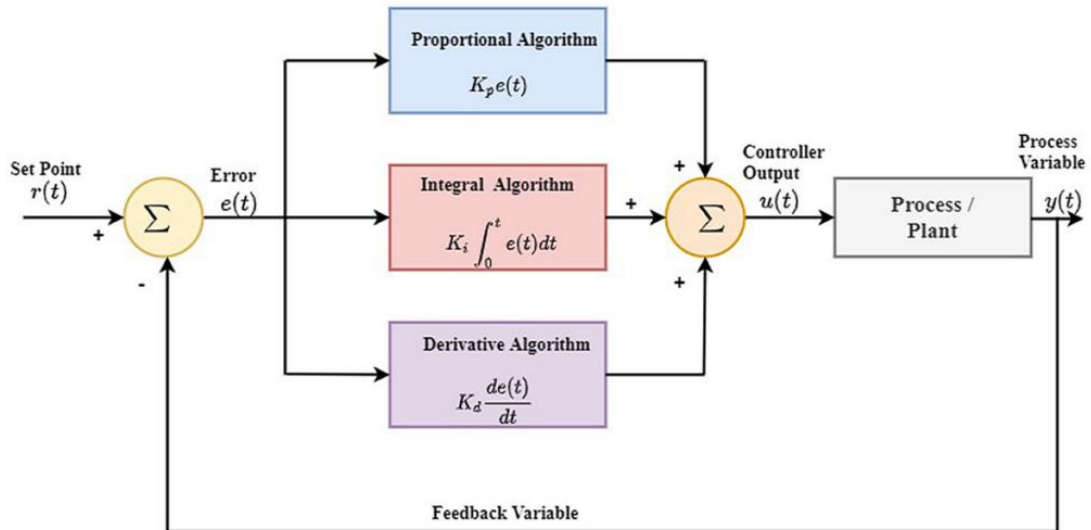


Figure 13: PID Controller Structure (Borase, 2020)

$R(t)$ is the state reference, $u(t)$ is the controller output (i.e., the yaw corrective moment M_z , for a Yaw Controller), $y(t)$ are the controlled states, like Yaw Rate and Side Slip Angle (Zanial, 2017).

K_p , K_i and K_d are the three tunable parameters that have to be modified in order to obtain the desired controller behavior and responsiveness. The simplest methodology to perform the controller tuning is the Trial and Error (Borase, 2020), knowing the effect of each parameter to the controlled system dynamic. Generally, the tuning starts with the proper choice of the proportional gain to obtain a desired responsiveness, then the integral gain is tuned to set the proper steady-state behavior, finally the derivative gain is set to fine-tune the transient dynamics.

For a Yaw Controller, this method can be performed on closed-loop maneuvers, with the target of minimizing lap-time or some costs functions, or in open loop maneuvers such as step steer or ramp steer, to better track the desired controller behavior.

2.2.2. Integral Sliding Mode Controller

The Sliding Mode Controller (SMC) is a Variable Structure Controller, which includes different functions that translates the plant states into a control surface. Generally, SMC exploits switching functions to switch from a control function to another one, with the target of changing the control sign, based on the control input. The threshold that defines the passage from one to another side is called sliding surface and its thickness is called boundary layer, useful to guarantee a smooth passage from the passage between different conditions. The control strategy works moving the system trajectory towards the sliding surface: the thickness of the boundary layer becomes the robustness tunable parameter.

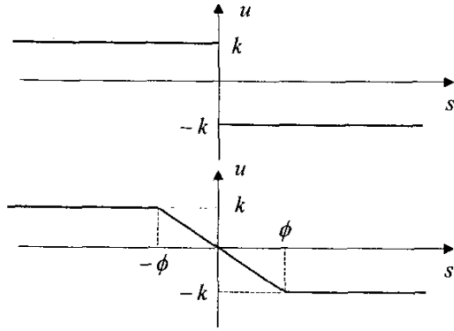


Figure 14: An example of sliding surface with its boundary layer (Goggia, 2015).

The Integral Sliding Model Controller (ISMC) (Goggia, 2015) is an evolution of the SMC that brings some advantages:

- ISM starts immediately with sliding motion, without the requirement of the reaching phase in which the system dynamic is not the ideal one.
- ISM can guarantee a smooth control action, through the first order filtering of the discontinuous control action, resulting in no chattering.
- ISM can be put in parallel with other simple controllers (i.e., constant gains PID controllers) to improve their steady state behaviour in extreme conditions.

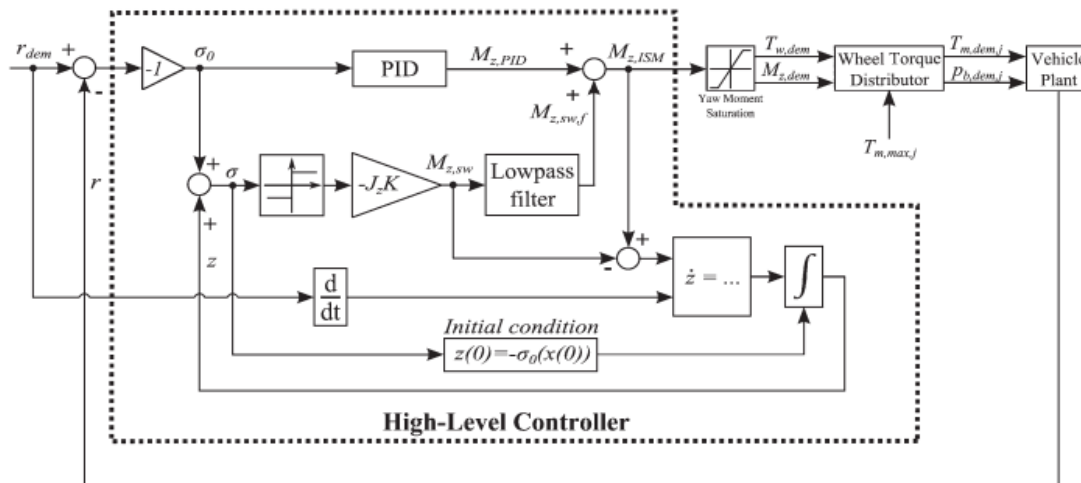


Figure 15: General ISMC structure for Torque Vectoring purpose (Goggia, 2015).

The tuning of the ISMC controller must be done considering three targets at same time:

- Asymptotic stability must be guaranteed for any working conditions. For this target, K is the only tunable parameter, that can be constant or gain-scheduled, based on an offline tuning.
- Chattering must be prevented since it will affect the tracking performance of the controller (for our application, this is clearly a bad feature, that let this controller become almost unapplicable in real time)
- Discontinuities or vibrations must be prevented to avoid damage in the electric powertrain and guarantee comfort. The last two targets can be fulfilled adjusting the time instant (τ_{ISM}) of the Lowpass Filter.

2.2.3. Fuzzy Logic Controller

The FL approach is based on a knowledge-based approach that exploits language variables. This permits an easier design of the controller when physical model is not present. With FL is possible to exploit fuzzy rules to derive a control action from the system inputs.

The general structure of a Fuzzy Inference System (FIS) is presented below, and it's characterized by three main blocks: fuzzification, interference engine and defuzzification.

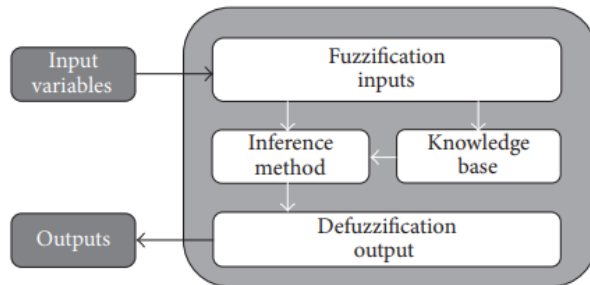


Figure 16: General diagram representing Fuzzy Logic approach (Parra Z. P., 2018).

The first and the last blocks are the responsible of translating a numerical variable into a fuzzy variable. They are performed through some membership functions sets. A fuzzy variable is a number that usually is comprised between 0 and 1. The most common membership functions are the triangular ones because of their simplicity and computational efficiency (Parra Z. P., 2018) .

An approach for FL controller applied to Yaw Control, is to have as control output the lateral torque distribution (i.e., the percentage of total torque given to the left side of the vehicle): during no torque vectoring action, this parameter will be 0.5. For extreme control actions, this parameter can achieve any value between 0 and 1.

The controller requires three inputs: Yaw Rate reference error, its derivative and Side Slip Angle reference error, based on a slip angle constant reference equal to zero rad to reduce understeering and improve handling.

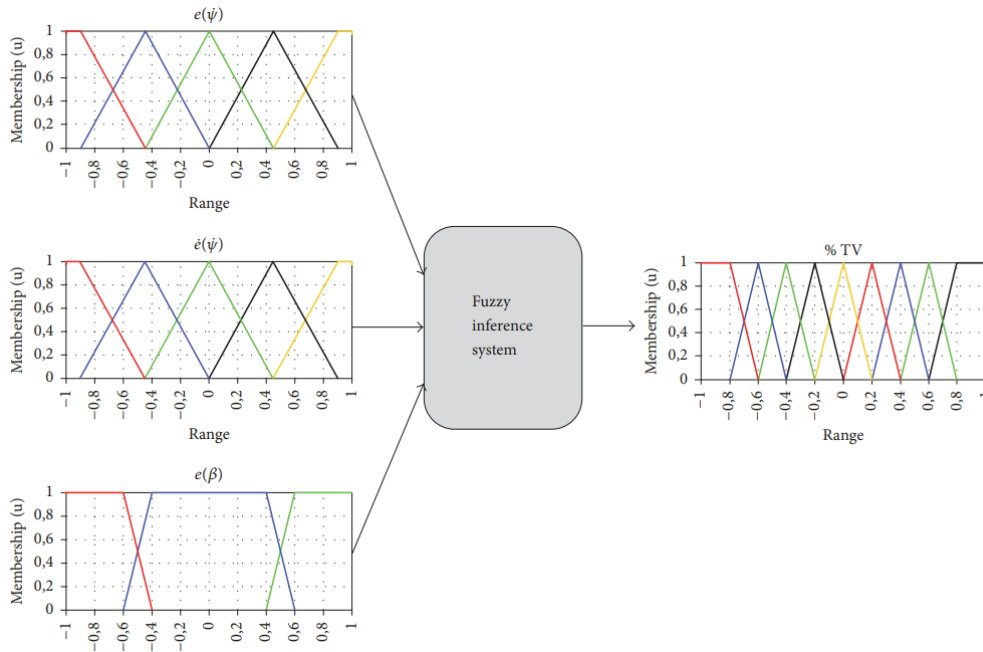


Figure 17: An example of FL based Yaw Control.

2.2.4. Linear Quadratic Regulator

A LQR controller is a full state feedback controller. This control strategy ensures good performances compared to previous analyzed strategies thanks to the possibility of minimizing (or eventually eliminating) the error by estimating the effectiveness of the solution by a cost function and a suitable gain (Tramacere, 2022), that can be achieved by solving iteratively the well-known Riccati equation for finite-horizon discrete time.

Being a model-based controller, it needs a vehicle model describing lateral vehicle dynamics. Moreover, a state space representation of that system is needed.

Together with that, a couple of weight matrices (Q and R) is needed to be defined by the user to stabilize the controlled system. Q matrix stabilize the system changing the states through state equation, R matrix instead acts on the control vector.

Both Q and R are scalar, positive, and symmetric matrices (Tramacere, 2022).

Assuming LQR to be able to control the system, maintaining it close to its equilibrium situation at each time instant, the vehicle model should be linearized at each time step, since models used to describe lateral vehicle dynamics may be highly nonlinear due to tire properties, aerodynamics.

In this way, the optimal feedback gain is updated at each time instant, depending on the dynamic evolution of the non-linear model.

Detailed description of a LQR control strategy is explained in chapter 3.

2.2.5. Feed Forward

Feed Forward control strategies, in contrary to feedback controllers, don't require any state feedback to perform actuation, so they work completely in open loop.

As every open-loop control strategy, system stability is not guaranteed and so, the controller cannot work alone, but it must work in parallel with any closed loop control strategy.

Anyway, some advantages still exist (Warth, 2019):

- Stability of closed loop system is not changed.
- Feed-forward can be designed and tuned independently from the other chosen parallel control strategy.
- System dynamics is improved thanks to the open loop controller.
- Feed forward controller is an additional controller tuning possibility to better control system dynamics.

Generally, feed forward works in transient maneuvers, while feedback controller guarantees stability in steady state conditions.

Detailed description of a Feed Forward control strategy is explained in chapter 3.

2.2.6. Model Predictive Control

The recent Control Science literature regarding Yaw Control, shows great interests in model-based control approaches with focus on Model Predictive Controls (MPC). A model-based controller heavily depends on mathematical equations representing the dynamics of the system.

The MPC works predicting the evolution of the system in a finite time period, called the prediction horizon and computes the control action depending on the reference(s) it has to track (Parra T. G., 2021).

Generally, due to the high non-linearities of the considered models for Yaw Control, such as dual track model for lateral dynamics and tire models, it is more common to implement Non-linear Model Predictive Controllers (NMPC).

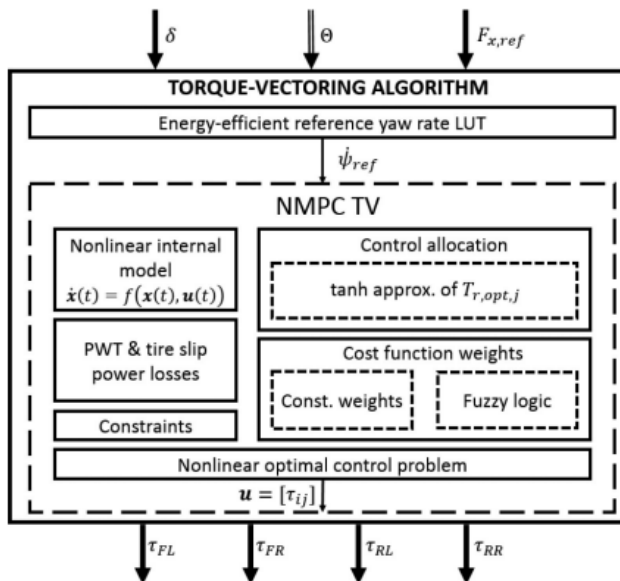


Figure 18: Simplified block diagram of the NMPC for Yaw Control (Parra T. G., 2021)

An example of the model that can be implemented is the dual track model, together with the dynamic model of each wheel, considering nonlinearities of tire-road interactions. The result

is a non-linear 7-DOF model with Speed, Yaw Rate, Side Slip Angle and the angular velocities of the four wheels as states.

At each time instant, the vector of states and measurements is fed to the controller as initial condition for the prediction model, then the prediction model will predict and optimize the future system behaviour. This optimization is achieved applying a control action at each time step a finite horizon optimization problem, using current state of the system, minimizing a cost function J , subject to some constraints.

Considering the application of this work, so a small, reactive race car, without a big ECU in which controller can be run, MPC cannot be employed. The best solution seems to be a parallel solution of

- LQR control for steady state stability, thanks to the accuracy of the model that can be achieved.
- Model-based feed-forward to improve vehicle's reactivity in transient manoeuvres.

3. Methodology

3.1. State Estimation

The implementation of a Yaw Controller requires signals that are generally not measurable with standard, low-cost, sensors. These quantities are mainly forces and angles that require respectively, for precise measurement, load cells and optical sensors, that, by now, are not available for the team.

In order to overcome this problem, some estimators can be implemented with the target of estimating tire forces in longitudinal, lateral and normal directions, tire slip angles and vehicle side slip angle. These estimators are necessary for the proper working of the Yaw Controller.

Every estimation performed in this chapter is compared with the output of the Vi-CarRealTime and Simulink co-simulation for validation, since Vi-CRT model is a high-fidelity digital twin of the team's vehicle. The chosen manoeuvre is a Skidpad (max performance event Vi-CarRealTime) since is at the same time a Formula SAE event and it contains both steady state and transient manoeuvres.

3.1.1. Vehicle States Estimation

Dual Track Model

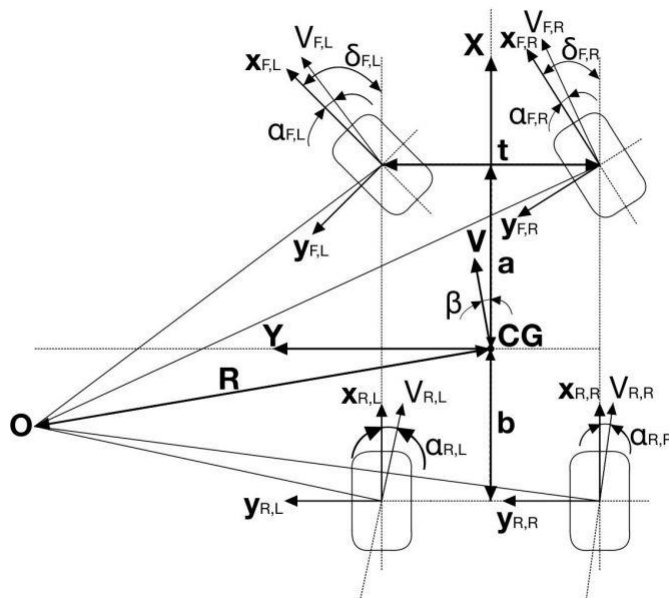


Figure 19: Dual Track Model

The vehicle model chosen to perform state estimation is the dual track model. In the automotive research and development field, using the Single-Track Model is generally more common, but for Formula SAE application, some of the hypotheses are not suited. Non-negligible values of track and wheelbase compared to typical competition curvature radii, together with the non-negligible load transfer during cornering manoeuvres, let impossible to collapse the outer wheels into a centre one to simplify the model.

Vehicle Side Slip Angle

The vehicle side slip angle, or attitude angle, is generally defined as the angle between the vehicle longitudinal axis and the vehicle CoG velocity vector [citazione Genta Morello vol2]. Its kinematic derivative has a precise physical definition (rajamani, 2009) (Giancarlo Genta, 2009):

$$\dot{\beta}_{kin} = \frac{a_{Y,Ch}}{V_x} - r + g \sin \phi_r$$

Unfortunately, the integration of this kinematic definition can be used for real-time side slip angle estimation only in simulation, where signals are not affected by noise. For real in-vehicle tests, signals are affected by asymmetric noise around nominal signal value, resulting in cumulative integration error and diverging side slip angle signal over time.

The estimation technique proposed in this thesis is a combination of discrete EKF-based estimation and kinematic-based estimation, i.e. the fusion of a discrete Extended Kalman Filter that estimates the side slip angle ($\hat{\beta}_{EKF}$) together with a kinematic-based approach that estimates its time derivative ($\dot{\beta}_{kin}$)

The discrete Kalman Filter, published for the first time by R.E. Kalman in 1960 is a recursive solution to the discrete data linear filtering problem (Welch, 2001), but if the process is nonlinear, Kalman filter's equations are no more valid. The Extended Kalman filter permits to linearize equations about current mean and covariance and its target is to estimate a state of a discrete-time controlled general process, with the approximated noise-free state equation:

$$\tilde{x}_k = f(\hat{x}_{k-1}, u_{k-1}, 0)$$

Using an approximated noise-free measurement equation that is

$$\tilde{z}_k = h(\tilde{x}_k, 0)$$

Since, from a computational point of view, a linear process is easier to be run in real time, these two equations can be linearized about the current approximated state and measure, becoming:

$$\begin{aligned} x_k &\approx \tilde{x}_k + A(x_{k-1} - \hat{x}_{k-1}) + Ww_{k-1} \\ z_k &\approx \tilde{z}_k + H(x_k - \tilde{x}_k) + Vv_k. \end{aligned}$$

W_{k-1} and v_k are random variables representing respectively process and measurement noises, that are generally assumed to be white and with normal probability distribution, meaning that means are zero and covariances matrices are known (Q and R , respectively). \hat{x}_{k-1} is the previous a-posteriori estimate. A is the Jacobian matrix of f with respect to x , W is the Jacobian matrix of “ f ” with respect to w , H is the Jacobian matrix of h with respect to x , V is the Jacobian matrix of v with respect to x .

From a high-level point of view, the discrete Kalman Filter algorithm works exploiting two operating stages: *time update* and *measurement update*. The first stage is responsible of projecting

in the future the current state and covariances, to obtain a-priori estimation of the states at the next time instant. The second stage is responsible of correcting the a-priori estimation, using the measurement equation, obtaining a more precise a-posteriori estimation. (Villano, 2021).

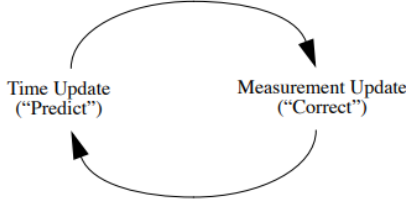


Figure 20: The Kalman Filter cycle

Going more in deep, the equations governing this cycle, and thus, the estimation, are five:

- Project the state ahead

$$\hat{x}_k^- = f(\hat{x}_{k-1}, u_{k-1}, 0)$$
- Project the error covariance ahead

$$P_k^- = A_k P_{k-1} A_k^T + W_k Q_{k-1} W_k^T$$
- Compute the Kalman Gain

$$K_k = P_k^- H_k^T (H_k P_k^- H_k^T + V_k R_k V_k^T)^{-1}$$
- Update estimate with measurement

$$\hat{x}_k = \hat{x}_k^- + K_k (z_k - h(\hat{x}_k^-, 0))$$
- Update error covariance

$$P_k = (I - K_k H) P_k^-$$

For this application of vehicle side slip angle estimation, the process equations are the ones solving equilibrium of a continuous time rigid-vehicle dual-track model on a road without any banking. The states to be estimated become at same time vehicle Side Slip Angle and Yaw Rate.

$$\begin{aligned} \dot{\beta} &= \frac{1}{m \cdot V} ((F_{x,FL} + F_{x,FR}) \cdot \sin(\delta) + (F_{y,FL} + F_{y,FR}) \cdot \cos(\delta) - (F_{x,RL} + F_{x,RR}) \\ &\quad \cdot \sin(\beta) + (F_{y,RL} + F_{y,RR}) \cdot \cos(\beta)) - \dot{\varphi} \\ \dot{\varphi} &= \frac{1}{J_z} ((F_{x,FL} + F_{x,FR}) \cdot l_f \cdot \sin(\delta) + (F_{y,FL} + F_{y,FR}) \cdot l_f \cdot \cos(\delta) - (F_{y,RL} + F_{y,RR}) \\ &\quad \cdot l_r + (F_{x,FR} \cdot \cos(\delta) + F_{y,FR} \cdot \sin(\delta) + F_{x,RR}) \frac{t}{2} - (F_{x,FL} \cdot \cos(\delta) \\ &\quad - F_{y,FL} \cdot \sin(\delta) + F_{x,RL}) \frac{d}{2} + MZ) \end{aligned}$$

The output vector, instead, is composed by Yaw Rate and the two axle lateral forces because, from literature, it is well known that this would improve the convergence speed of estimation.

$$Z = [\dot{\varphi}, F_{y,F}, F_{y,R}]^T$$

Since both front and rear axle forces are used as output vector, they must be used as measurement as well, starting from IMU signals. Since geometry and inertias are known and IMU signals are considered reliable, we can use estimated forces as measurements.

$$\hat{F}_{yF} = \frac{ma_y l_R + I_z \dot{r}_{meas}}{l_F + l_R}$$

$$\hat{F}_{yR} = \frac{ma_y l_F - I_z \dot{r}_{meas}}{l_F + l_R}$$

Then, EKF-based estimation and kinematic formulation are put together to improve the final estimation, using a time constant $\tau = 10/(2\pi)$ (rajamani, 2009).

$$\hat{\beta} = \frac{1}{\tau s + 1} \hat{\beta}_{EKF} + \frac{\tau}{\tau s + 1} \dot{\beta}_{kin}$$

Tire Slip Angle

The tire slip angle is a similar concept compared to the vehicle side slip angle but translated to the tire reference frame. The slip angle is, by definition, the angle between the tire velocity vector and the X axis of its own reference frame. From a physical point of view the tire slip angle is the necessary relative deformation needed to generate and exchange force with the ground. From this perspective the tire slip angle is a fundamental parameter to control vehicle handling.

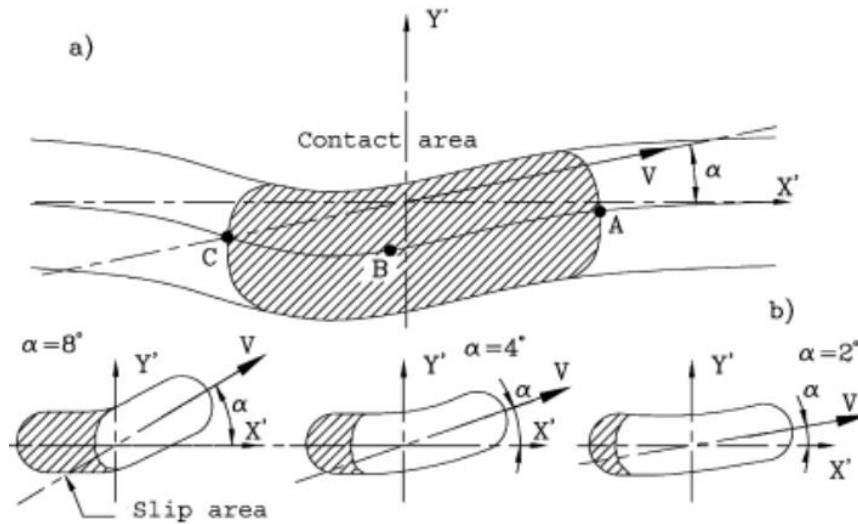


Figure 21: Tire Slip Angle (Genta & Morello, 2020)

From kinematic analysis of the dual track model, it is possible to derive formulae for the slip angle of each tire.

$$\alpha_{front,i} = \arctan\left(\frac{V_y + rx_i}{V_x - ry_i}\right) - \delta_i$$

$$\alpha_{rear,i} = \arctan\left(\frac{V_y + rx_i}{V_x - ry_i}\right)$$

Figure 22: Tire Slip Angle comparison

Tire Forces

The estimation of tire forces is of prior importance in vehicle dynamics control strategies, like Yaw Control. In this application it is fundamental to know normal forces for the knowledge of the axle cornering stiffness and lateral forces since they are used as added measurement in the EKF for the Side Slip Angle estimation.

Tire Normal Force

Starting from the normal force estimation, for a rigid vehicle, they depend mainly on three different contributions: static vehicle and driver load, vehicle and driver load transfer and aerodynamic forces (Giancarlo Genta, 2009).

$$F_{z,static,i} = mass \cdot g \cdot weight_{\%,i}$$

$$\Delta F_{z,long} = \frac{mass \cdot a_x \cdot h_{CoG}}{l}$$

$$\Delta F_{z,lat} = \frac{mass \cdot a_y \cdot h_{CoG}}{t}$$

$$F_{z,aero} = \frac{1}{2} C_z \cdot \rho_{air} \cdot V_x^2 \cdot A \cdot Aero_{\%,i}$$

Tire Longitudinal Force

Longitudinal forces exchanged between tire and ground are generated from a local deformation of the tires, called longitudinal slip. The trend of the longitudinal force as function of the longitudinal slip is highly non-linear and a precise theorization has been proposed by Hans B. Pacejka in early 90's. The most common formulation of a Magic Formula is the following (Pacejka, 2002):

$$F_{x0} = D_x \sin[C_x \arctan\{B_x K_x - E_x (B_x K_x - \arctan(B_x K_x))\}] + S_{Vx}$$

Where all B, C, D, E, S are the combination of many other coefficients that can be found on standard “.tir” files, obtained from experimental test bench data fitting. K_x , instead is the longitudinal slip.

Typical trends for Longitudinal Force versus longitudinal Slip are reported below as function of the normal load acting on the tire.

The proposed trends are based on the so-called Magic Formula MF6.2 that considers as input variables tire normal force, longitudinal slip, slip angle, camber angle and pressure.

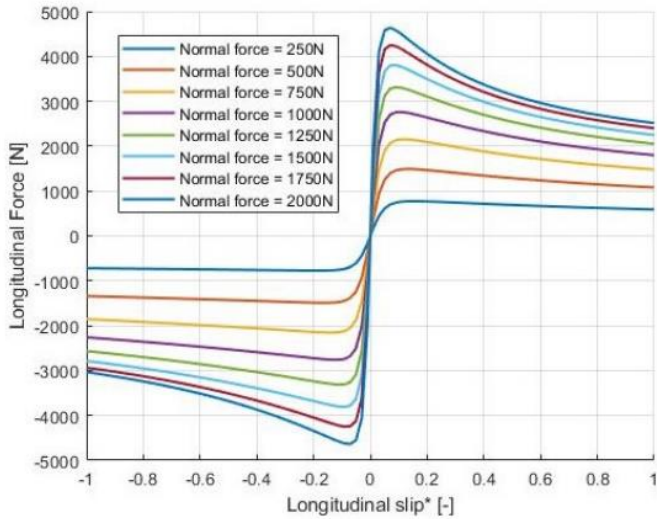


Figure 23: Tire Longitudinal Force (Magic Formula 6.2)

Tire Lateral Force

The estimation of the tire lateral force is like the estimation of the tire longitudinal force, with the difference that the tire deformation that guarantees the force transmission is an angular deformation and it is the slip angle. For the estimation of the lateral force, the same inputs of the longitudinal force are necessary (normal load, slip angle, longitudinal slip, camber angle, pressure and wheel velocity)

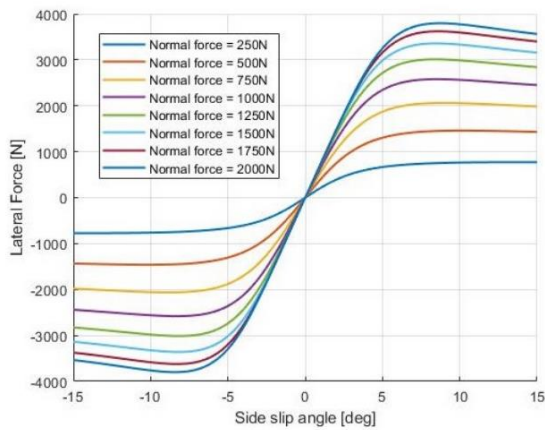


Figure 24: Tire Lateral Force (Magic Formula 6.2)

3.2. Yaw Control

3.2.1. A-LQR

In this work the feedback Yaw Controller implemented is an Adaptive-LQR, that from literature is a good compromise between performance and computational effort. The A-LQR takes input from the driver (Steering, accelerator, and braking inputs) and feedbacks from vehicle dynamics sensors or estimates (Speed, Longitudinal and Lateral accelerations, Yaw Rate, Side Slip Angle).

The implemented vehicle model is, as for the Side Slip Angle EKF, a dual track rigid vehicle model. Tire forces are modelled through a complete Pacejka Magic Formula 6.2.

$$\dot{\mathbf{x}} = f(\mathbf{x}, \delta_F, v_x, a_x, a_y) + B_u u$$

The dynamic of the model depends on the states themselves (Side Slip Angle, Yaw Rate) and on the input u , i.e., the corrective Yaw Moment (M_z). Longitudinal velocity V_x , Longitudinal acceleration, Lateral acceleration are considered as lumped time-varying parameters, while the driver steering input is considered as the main disturbance of the controlled system (Manca, Molina, Hegde, Tonoli, & Amati, 2023).

Being the A-LQR a feedback controller, it must react to an error, that in this case it will be called reference error. This error is generally computed as the difference between a reference and a measured (or estimated with sufficient accuracy) quantity. In this case, the references are both the Yaw Rate and the Side Slip Angle.

The first reference is computed through steady state understeering characteristic formula:

$$\dot{\phi}_{ref,ss} = \frac{V_x \delta_F}{\alpha_1 l (1 + K_{US} V_x^2)}$$

$$\dot{\phi}_{max} = \frac{\mu g}{V_x}$$

Where K_{US} is the understeering coefficient and α_1 is a tuneable parameter to improve the overall responsiveness of the desired ideal vehicle.

Reference Side Slip Angle is instead computed as:

$$\beta_{ref,ss} = \beta_{max} \tanh\left(\frac{\beta}{\beta_{max}}\right)$$

$$\beta_{max} = \text{atan}(0.02 \mu g)$$

The implemented A-LQR aims to improve the steady state behaviour of the controlled vehicle, and, as said before it is based on a dual track vehicle model, with fully non-linear tires. Due to this reason, the system must be linearized at each time instant about its working point, exploiting Jacobian formulations. Jacobian matrices must be computed at each time step since states, inputs and parameters are time-varying.

$$\dot{\mathbf{x}} = J_A \mathbf{x} + J_{BD} \delta_F + J_{Bu} u$$

Where u , the control input, i.e., the corrective Yaw moment is computing minimizing the following cost function:

$$J = \int_0^{\infty} (\mathbf{x}^T \mathbf{Q} \mathbf{x} + u R u) dt$$

With the weight matrices that are adapting to the maximum values the states and the control variable can achieve at that time step:

$$\mathbf{Q} = \begin{bmatrix} \frac{1}{\beta_{max}^2} & 0 \\ 0 & \frac{1}{\dot{\psi}_{max}^2} \end{bmatrix}$$

$$R = \frac{1}{M_{z,max}^2}$$

Maximum control variable is defined just from tire dynamics and geometry, giving the following formulation:

$$M_{z,max} = \frac{t w_F}{2} |F_{x,FR,max} - F_{x,FL,max}| + \frac{t w_R}{2} |F_{x,RR,max} - F_{x,RL,max}|$$

Where $F_{x,ij,max}$ are the maximum longitudinal force each tire can exert at any time instant, considering both maximum motor torque and force obtained at maximum tire slip. Finally, the control action is given by:

$$M_{z,LQR} = \mathbf{K}_{LQR} \begin{pmatrix} \beta_{ref} - \beta \\ \dot{\psi}_{ref} - \dot{\psi} \end{pmatrix}$$

3.2.2. Model-Based Feed Forward

For this application, the steady state behaviour is not the only indicator of performance since reactivity of the controlled system is a key indicator as well. For this reason, a feedback controller alone is not sufficient in guaranteeing both good steady state behaviour and necessary speed of response.

An open loop contribution become, in this way, necessary to fulfil the second requirement (i.e., the responsiveness of the system).

The feed-forward become the controller contribution to behave in a more agile manner, while the Λ -LQR becomes the main contribution during steady state manoeuvres.

The feedforward is expressed in frequency domain, following Laplace notation:

$$FF(s) = \frac{M_{z,FF}(s)}{\delta_F(s)} = \frac{G_{des}(s) - G_{nom}(s)}{G_p(s)}$$

$$G_{des}(s) = \frac{\dot{\psi}_{des}(s)}{\delta_F(s)}, G_{nom}(s) = \frac{\dot{\psi}(s)}{\delta_F(s)}, G_p(s) = \frac{\dot{\psi}(s)}{M_{z,FF}(s)}$$

Where G_{nom} , G_{des} and G_p are all transfer functions, respectively between nominal vehicle yaw rate and steering input, desired vehicle yaw rate and steering input and nominal vehicle yaw rate and yaw moment input.

With “desired vehicle” it’s intended a vehicle with less J_z inertia moment (for example, 75% of the nominal inertia moment).

All the transfer function are related to the dual track model presented above, but in this case with linear tire behaviour, with constant cornering stiffness, to improve speed of response and reduce ripple in feed-forward output.

The bode diagram of the Feed Forward action transfer function has been investigated, to understand the Feed Forward action output as function of the steering angle input. The sensitivity analysis has been performed as function of the Velocity and the Desired Inertia Moment about Z axis of the vehicle (J_{z^*})

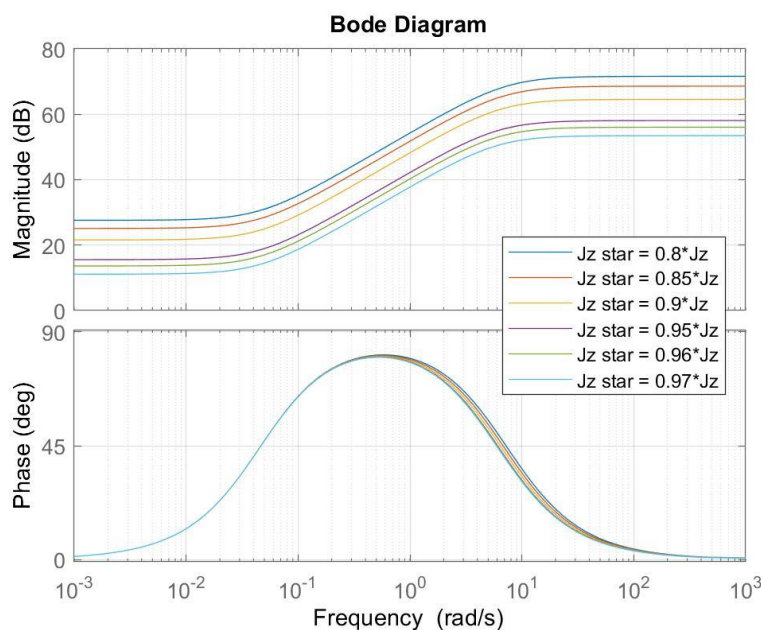


Figure 25: Bode Diagram of $FF(s)$ varying Desired Inertia Moment

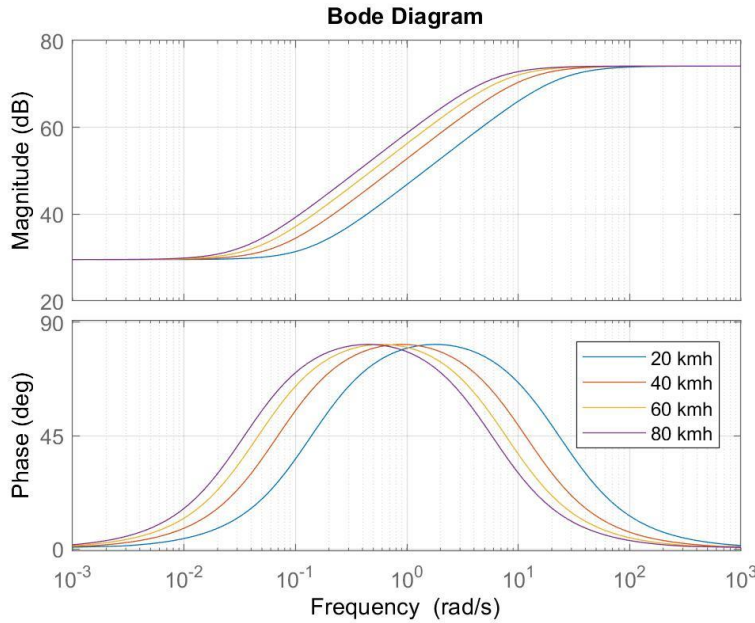


Figure 26: Bode Diagram of $FF(s)$ varying Vehicle Longitudinal Speed

Figure 17 represents the Feed Forward bode diagram varying the ratio between Yaw Inertia moment of the real and desired vehicle. The Yaw Inertia moment is the vehicle parameter that most influences the reactivity during transient cornering manoeuvres, being inversely proportional to the Yaw Acceleration. Due to that the ratio between desired and real Yaw Inertia moment becomes the only tuning parameter of the Feed Forward controller. It can be seen how, increasing the divergence between the reference and real inertia moment, the magnitude increases at all frequencies. This represents an increase of controller actuation, since more M_z is needed to match the real and desired vehicle behaviour, with same boundary conditions.

Figure 18, instead, represents the Feed Forward bode diagram at different vehicle velocities, the only varying, non-controllable parameter of the system. It can be noted that, increasing the corner entry speed, the controller actuation increases, for the same input frequency. In practice, a more confident driver will be helped more by the Feed Forward.

3.3. Motor Torque Allocation

After having computed the desired M_z , the way in which the Torque Vectoring logic can deliver such M_z to the vehicle is thanks to a motor torque unbalance between the left and right sides of the vehicle. Such torque unbalance will generate tire longitudinal force unbalance, too. That unbalance will generate the required M_z coming from the upper-level controller.

The assumption of the implemented torque allocation is to generate such M_z thanks to a symmetric motor torque adjustment, called ΔT_{mot} . ΔT_{mot} will be added or subtracted as the same quantity between the left and right part of the same axle to guarantee the same total motor torque per each axle. In this way, the understeering/oversteering characteristics of the vehicle is not changed, since both axles will still deliver the same amount of motor torque.

$$M_z = Fx_{FR} \frac{t_f}{2} - Fx_{FL} \frac{t_f}{2} + Fx_{RR} \frac{t_r}{2} - Fx_{RL} \frac{t_r}{2}$$

$$Fx_{ij} = \frac{(T_{mot} + \Delta T_{mot})}{R_{ij}}$$

$$M_z = \frac{(\Delta T_{mot}) t_f}{R_{ij}} \frac{1}{2} - \frac{(-\Delta T_{mot}) t_f}{R_{ij}} \frac{1}{2} + \frac{(\Delta T_{mot}) t_r}{R_{ij}} \frac{1}{2} - \frac{(-\Delta T_{mot}) t_r}{R_{ij}} \frac{1}{2}$$

From the last equation, ΔT_{mot} can be obtained and given as same quantity as addition or subtraction on the same axle. In order to know where to add and where to subtract, it's sufficient to look at the sign of the requested M_z . Positive M_z means help the vehicle to rotate faster counterclockwise, while negative M_z means help the vehicle to rotate faster clockwise.

In the first case, the ΔT_{mot} will be added to the right wheels, while in the second case to the left wheels.

4. Numerical Results

4.1. Vi-CarRealTime

Every simulation for this work has been performed exploiting Matlab-Simulink and Vi-CarRealTime co-simulation.

Vi-CarRealTime is defined by Vi-Grade, the company owner of such software, as a “virtual modelling environment targeted to a simplified four wheels vehicle model”. The potentiality of Vi-CarRealTime is the ease of recreating a digital twin of every real vehicle, just inserting in the software known physical parameters for every main subsystem of the vehicle. Then the digital twin is generated assembling each subsystem, but this operation is automatically performed by the software. This way of simulating may be difficult for existing vehicle, where data are OEM’s secrets, but for FSAE vehicles, and prototypes in general, where the simulation team is strictly in contact with design team is very convenient since every vehicle parameter is decided and studied together.

Every digital twin of a FSAE electric vehicle on Vi-CarRealTime, and so the Squadra Corse PoliTo one as well, is characterized by:

- Mass and its distribution of sprung, unsprung, driver masses
- Measured or CAD estimated full vehicle inertia.
- Real vehicle geometrical parameters: wheelbase length, CoG coordinates, tracks widths, centre of pressure position, etc
- Aerodynamic Forces (front lift, rear lift, drag) look-up tables in function of front and rear ride heights as results of CFD models or wind tunnel tests.
- Full front, rear suspensions and steering system elasto-kinematic model developed in MSC Software Adams Car environment and imported through the dedicated GUI
- Full powertrain model: motors coordinates and inertias, traction and braking torque and efficiency map as function of speed, transmission ratio and efficiency.
- HV battery model
- Tire model: Pacejka Magic Formula 6.2 with data coming from dedicated Pirelli .tir file, obtained from tire test rig data fitting
- Mechanical braking system with real data: number of pistons, friction coefficient, geometry, inertia.

Vi-CarRealTime simulation is divided mainly in two types of events: standard manoeuvres and max performance manoeuvres.

Standard manoeuvres represent the common benchmarks manoeuvres for the automotive industry, defined by precise actions from the driver, generally in open loop: straight acceleration, straight braking, acceleration in turn, braking in turn, ramp steer, step steer, sine steer, moose test, etc.

Max performance events, instead, are closed loop manoeuvres, generally performed on specified tracks imported using two different files: .drd files defining the shape of the track and .rdf files defining the road characteristic like roughness, friction coefficient, bumps, etc. Every track is subdivided in small sectors that the driver model must perform without any loss of control. Loss of control is reached during these events when the maximum distance from the centreline, defined as input by the user, is overcome. In case of loss of control in a particular part of the track, the driver model must redo the sector applying up to three actions: reduction of Longitudinal Performance Factor, reduction of Lateral Performance Factor, reduction of braking Performance factor. Performance Factors (PF) are tuneable

parameters by the user representing the ‘aggressiveness’ of the driver during acceleration, cornering, and braking. Over-aggressiveness may conduct to loss of control and a reduction of these parameters is the only way to fulfil a certain sector.

When a sector must be redone with lower PF, Vi-CRT calls it “iteration”. It is clear how the number of iterations to complete a certain track can be a useful KPI when comparing the same vehicle equipped with different controllers. The lower the number of iterations, the smoother the controller behaviour is, since the driver model can perform the same track with higher PF.

Vi-CarRealTime | Simulink co-simulation environment

Since Vi-CarRealTime is a software for vehicle modelling, the equipped control system for motor torque control is very basic. In fact, Vi-CRT assumes a constant torque repartition between front and rear axles, from user input.

When a more sophisticated torque control strategy is necessary, it can be developed on Simulink and put in co-simulation with Vi-CRT environment.

Vi-CRT permits to import into Simulink the complete vehicle model, the driver model, and the manoeuvre to be performed: in this way the four motor torques, that generally are the outputs of a vehicle dynamic control system, become the input of the Vi-CRT model and the vehicle dynamics can be properly controlled.

As output, the Vi-CRT model gives a bus with hundreds of vehicle states signals, like chassis accelerations, velocities and displacements, wheels accelerations and velocities, vehicle side slip angles, tire slips and slip angles, battery state of charge, suspensions displacements, ride heights and so on.

Being the number of existing signals so high, way higher than the ones existing on the real vehicle, this co-simulation can be also used to develop and tune estimators for signals requiring big or expensive sensors.

4.2. Key Performance Indicators (KPIs) Definitions

To evaluate the performance improvement of a lateral vehicle dynamics controller under development, some KPIs are listed in literature. A KPI is a tool that aims to evaluate, numerically, and in a direct way, the behaviour of a certain system. The selected KPIs for this work are the following:

$$Yr_cost = \int_{t_0}^{t_{fin}} (|Yr_{actual} - Yr_{reference}|) dt$$

$$Beta_cost = \int_{t_0}^{t_{fin}} (|\beta_{actual} - \beta_{reference}|) dt$$

The first, represents the cumulative deviation of the Yaw Rate compared to the neutral vehicle ideal Yaw Rate.

The second, represents the cumulative deviation of the Side Slip Angle compared to the reference value, as described in chapter 2.3.

For both equations, a reduction of the integral value, and so, of the KPI, represents a reduction of signals overshoot, oscillations, and steady state error, since these integrals represent, from a mathematical point of view, the absolute value of the area of the two states errors.

From a physical point of view, instead, a reduction of cost functions means a more neutral, nominal behaviour, resulting in a more driveable and performing vehicle. The reduction of these two KPI has been a key point during controller tuning.

4.3. Standard Manoeuvres

Being the controller under development aimed to improve both steady state and transient manoeuvres, the selected standard events are chosen to underline improvements separately. The tuning of the A-LQR has been done in constant radius cornering and ramp steer, being the manoeuvres quasi-steady state, the contribution of the Feed Forward is at its minimum. The tuning of the Feed Forward has been done in sine sweep steer, being the manoeuvre highly transient, its contribution is at its maximum, while the A-LQR contribution is at its minimum, since there is no sufficient time to let the steady state actuation to rise.

On every manoeuvre, a sensitivity analysis for the selection of the best Torque Vectoring tuning parameters has been done with trial and error in order to minimize cost functions and maximize performance. In the following analysis the comparison between the best tuned Torque Vectoring and vehicle equipped only with Traction Control is proposed in order to underline the TV improvements.

With this target, the events under investigation are the following.

Constant Radius Cornering

- External Corner Radius: 9 m
- Radius Width: 3 m
- Initial Speed: 5 m/s
- Final Speed: 12 m/s

The geometry of the corner has been selected as the most challenging FSAE hairpin turn from Autocross Track Layout. The selected final speed is the one guaranteeing theoretical 1.5g of lateral acceleration (low speed grip limit for Pirelli tires).

Ramp Steer

- Constant Speed: 20 m/s
- Initial Steering Angle: 0 deg
- Final Steering Angle: 40 deg
- Steering Rate: 10 deg/s
- Manoeuvre start time: 1 s

The speed and steering angles have been selected considering the average situation of standard FSAE corners.

Sine Sweep Steer

- Constant Speed: 10 m/s
- Steering Amplitude: 15 deg
- Initial Steering Frequency: 0.01 Hz
- Final Steering Frequency (for performance evaluation): 3 Hz
- Final Steering Frequency (for Bode Diagram): 100 Hz

The steering amplitude has been selected as the angle guaranteeing lateral acceleration of 1 g in Ramp Steer Manoeuvre.

4.3.1. Constant Radius Cornering

State Estimation

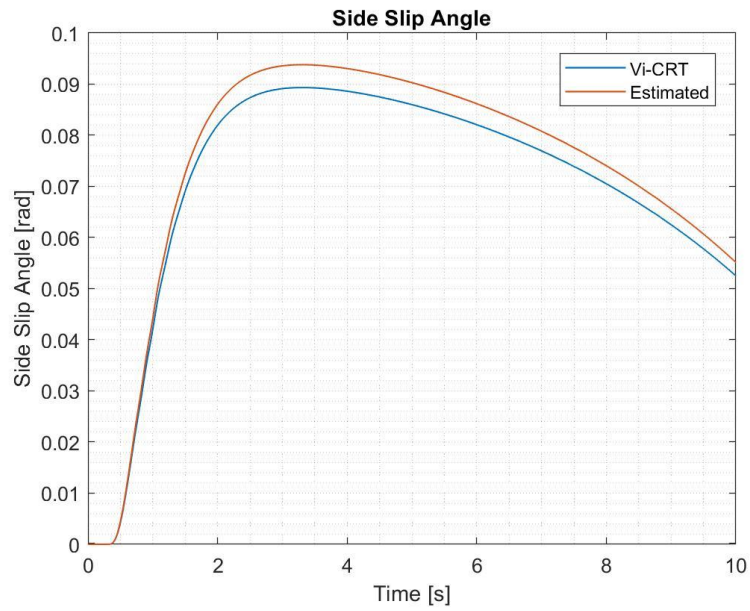


Figure 27: Side Slip Angle Estimation vs Vi-CRT output (constant radius cornering) – RMS error = 0.00312 rad

Yaw Control

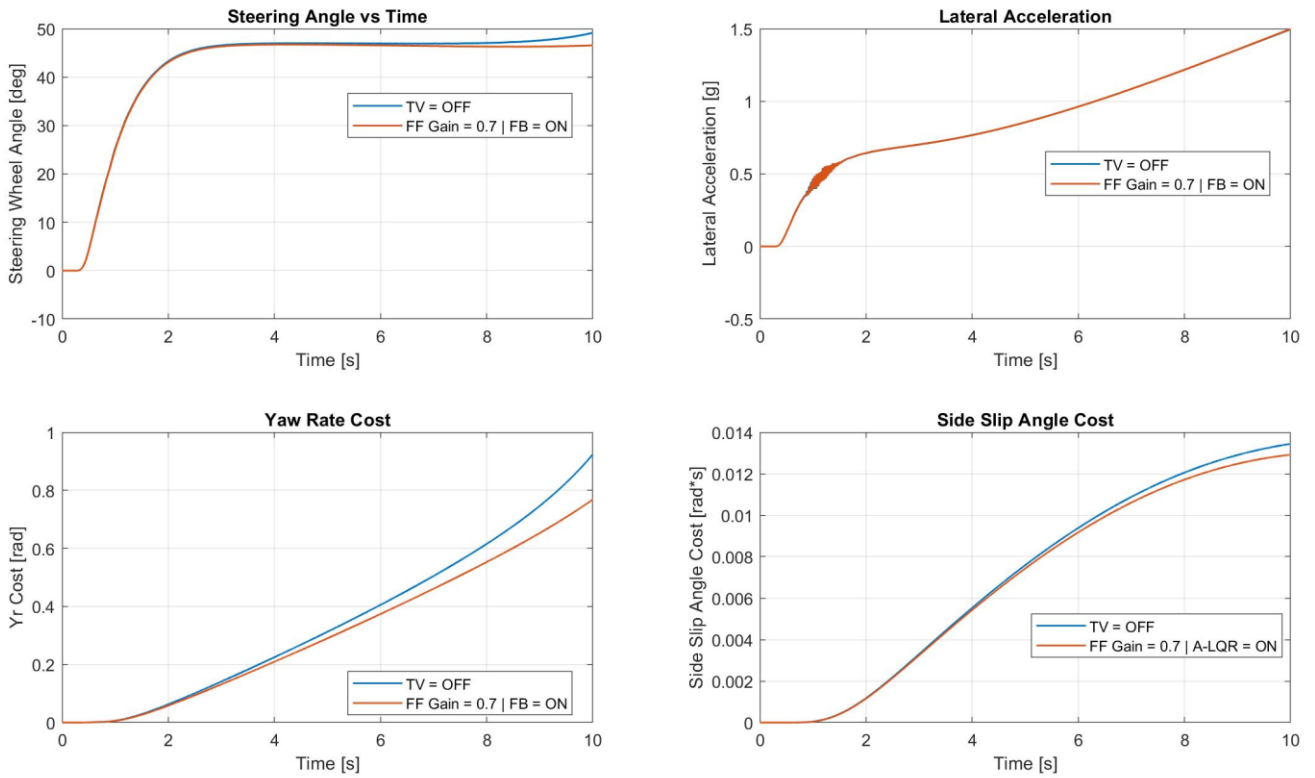


Figure 28: Lateral Characteristic Comparison in Constant Radius Cornering for TV OFF and TV ON

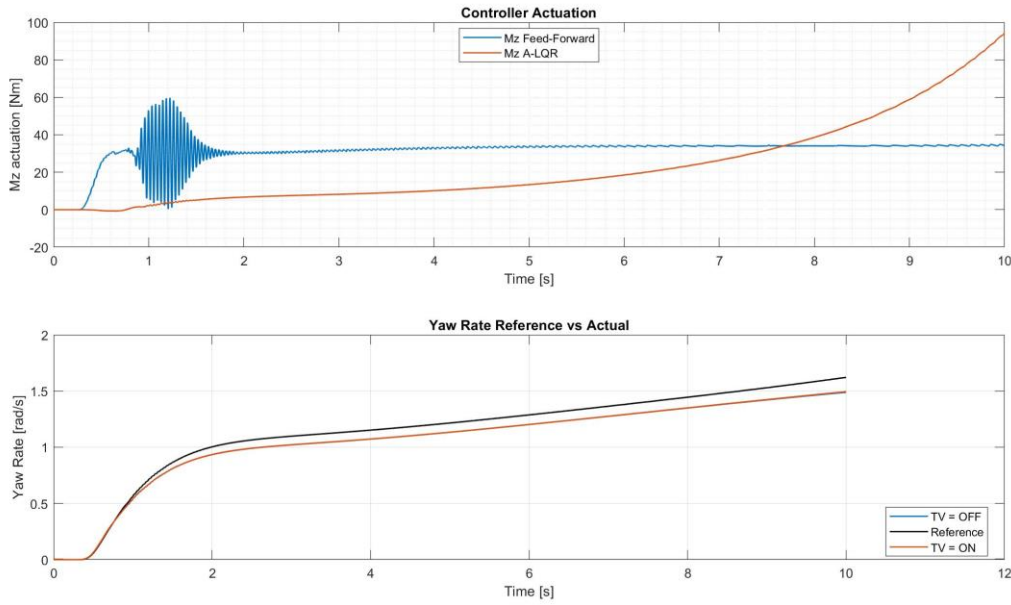


Figure 29: Controller Actuation and Yaw Rate trends for Constant Radius Cornering maneuver

Estimation is good, no divergence occurs. Steady state tracking is guaranteed, and transient side slip angle ramp estimation is precise.

RMS error between estimated and Vi-CRT remains low, at 0.00312 rad.

What is interesting to note is that, even if the lateral acceleration trend with time is almost the same, the Steering Angle needed to run that corner, with that speed trend, can remain more constant as speed increases, demonstrating a reduction of understeering behavior of the controlled vehicle. At same time, both the Yaw Rate and Side Slip Angle costs, are reduced. The manoeuvre, overall, is not very challenging and so the beneficial effect is limited.

Also, it can be noted that the actuation of the controller is very limited for both contributions, with minimum and almost constant Feed Forward contribution (this is the expected result from the amplitude of the Bode diagram: at almost zero steering frequency the actuation is at its minimum, constant, but not zero). The A-LQR contribution, instead is almost zero in the starting phase of the manoeuvre, when the divergence between desired and actual Yaw Rate is very small. It increases in the final part of the corner, where the tire non-linearities kick in and the vehicle behavior starts to diverge from the ideal one. Increasing more the speed of that corner would result in highly understeering behavior from 11 m/s on, losing all the sense of the analysis.

	Yaw Rate Cost	Side Slip Angle Cost
TV = OFF	0.911	0.0137
TV = ON	0.782	0.0129

Table 2: Numerical Comparison of State Costs with TV = OFF and TV = ON

Torque Allocation

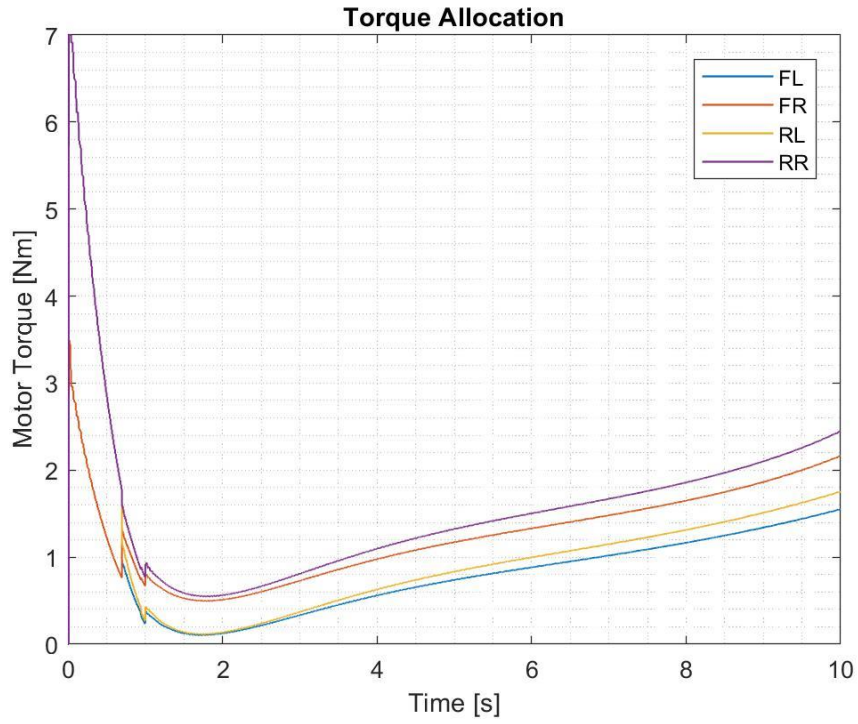


Figure 30: Torque Allocation – Constant Radius Cornering

Torque allocation trend is good, profiles are smooth along all the corner, small oscillation occurs during corner entry, when Fedd forward actuation has small oscillations, too.

4.3.2. Ramp Steer

State Estimation

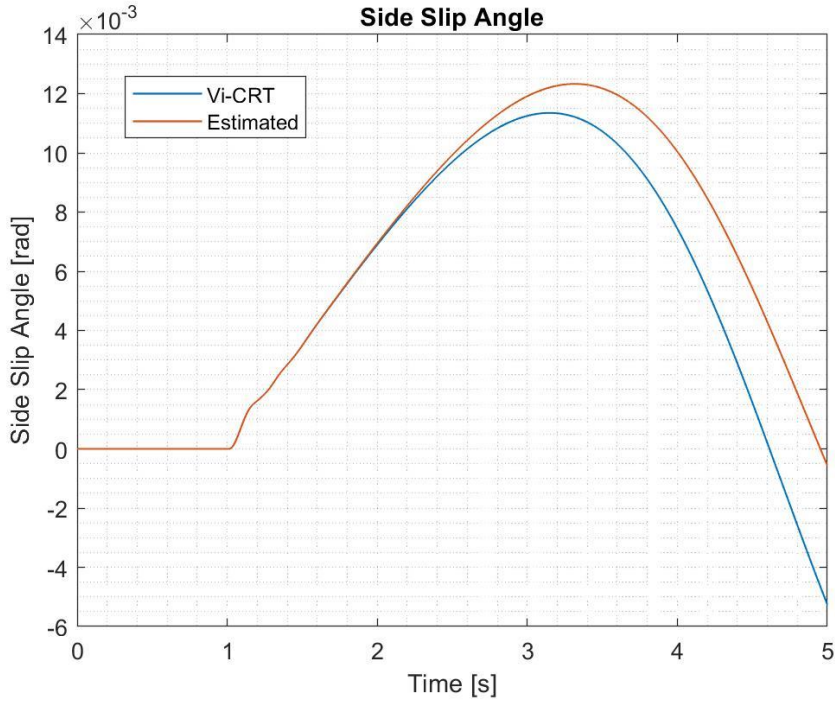


Figure 31: Side Slip Angle estimation vs Vi-CRT output (ramp steer) – RMS error = 0.00147 rad

Yaw Control

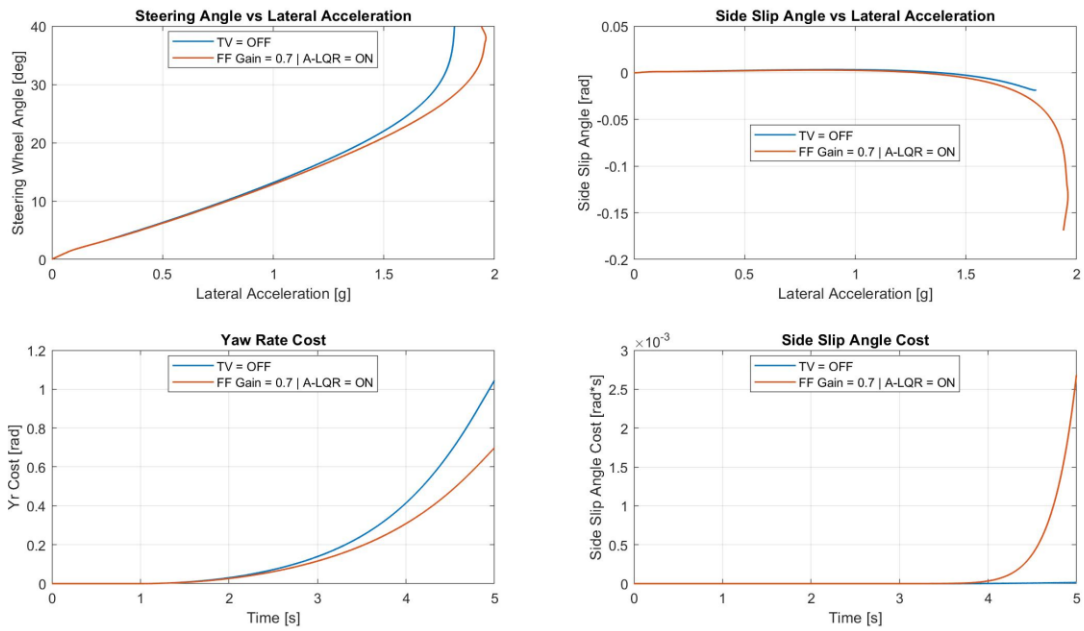


Figure 32: Lateral characteristic comparison in Ramp Steer with TV = OFF and TV = ON

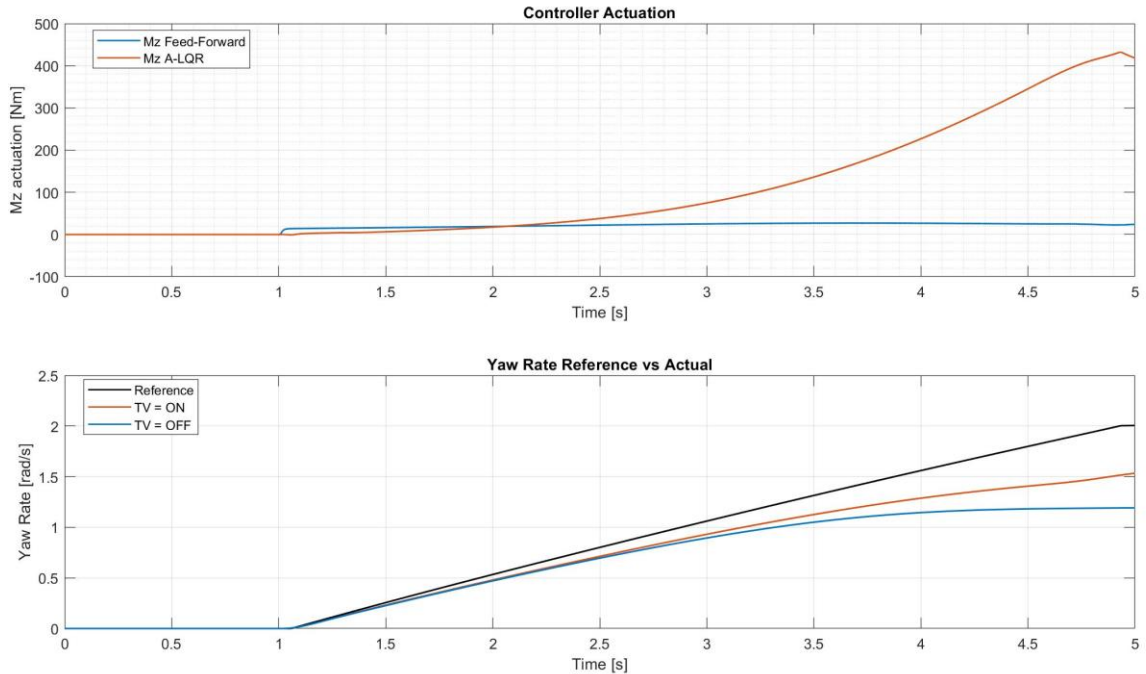


Figure 33: Controller actuations and Yaw Rates (ramp steer)

Estimation is good, no divergence occurs. Steady state tracking is guaranteed, and transient side slip angle ramp estimation is precise.

RMS error between estimated and Vi-CRT remains low, at 0.00147 rad.

For this kind of maneuver, instead, improvements are noticeable. The vehicle equipped with complete and tuned Torque Vectoring exhibits higher lateral acceleration performances, increased linear relation between Steering Angle and lateral acceleration and an overall reduced understeering characteristic.

The last can be noted both for the slightly reduced slope in linear part of the top left plot, but also for the Side Slip angle trend with lateral acceleration. At very high lateral accelerations ($> 1.7 g$) a small oversteer has been induced. Being the maneuver boundary conditions the same for both vehicles (same speed and same steering angle trend), all improvements can be addressed to the Torque Vectoring introduction.

	Yaw Rate Cost	Side Slip Angle Cost
TV = OFF	1.052	0.000112
TV = ON	0.692	0.00273

Also, it can be noted that the Feed Forward actuation is as its minimum and totally negligible compared to the A-LQR: this is because, being a quasi-steady state manoeuvre, its frequency actuation is not triggered, exactly as before. On the other hand, since this manoeuvre achieves high non-linear regions of the vehicle dynamics, big separation occurs between Reference and actual Yaw Rates, inducing the A-LQR to give a lot of actuations.

Yaw Rate trend of the controlled vehicle is always above the Yaw Rate of the uncontrolled vehicle, meaning that the first can rotate faster about its Z axis. This is a clear indicator of better lateral performance.

Torque Allocation

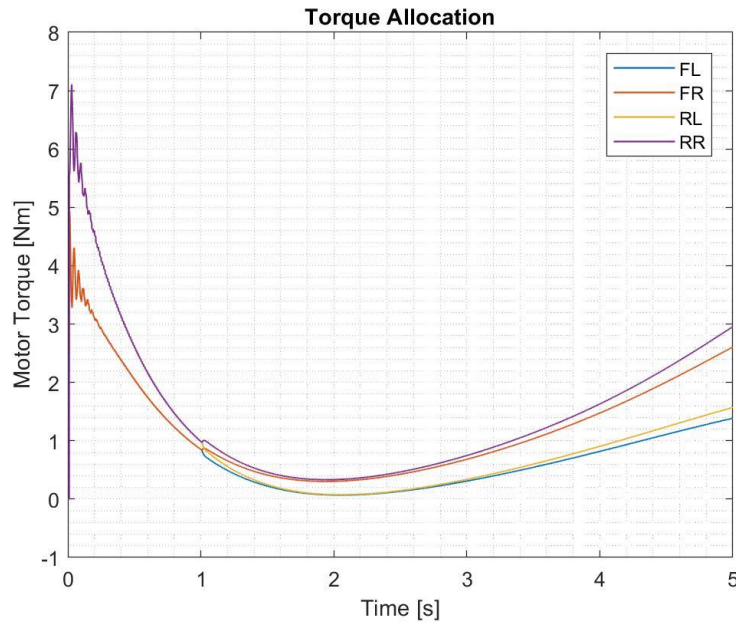


Figure 34: Torque Allocation (ramp steer)

Torque allocation trend is good, profiles are smooth along the corner. No oscillations occur, compared to the previous manoeuvre. The torque unbalance increases, time step after time step, because the vehicle progressively leaves linear tires dynamics region, entering the nonlinearities region. For this reason, the vehicle progressively becomes more and more understeering, due to front axle saturation first, and the measured Yaw Rate diverges from the ideal yaw rate. The result is a progressively torque unbalance along the manoeuvre.

4.3.3. Sine Sweep Steer

State Estimation

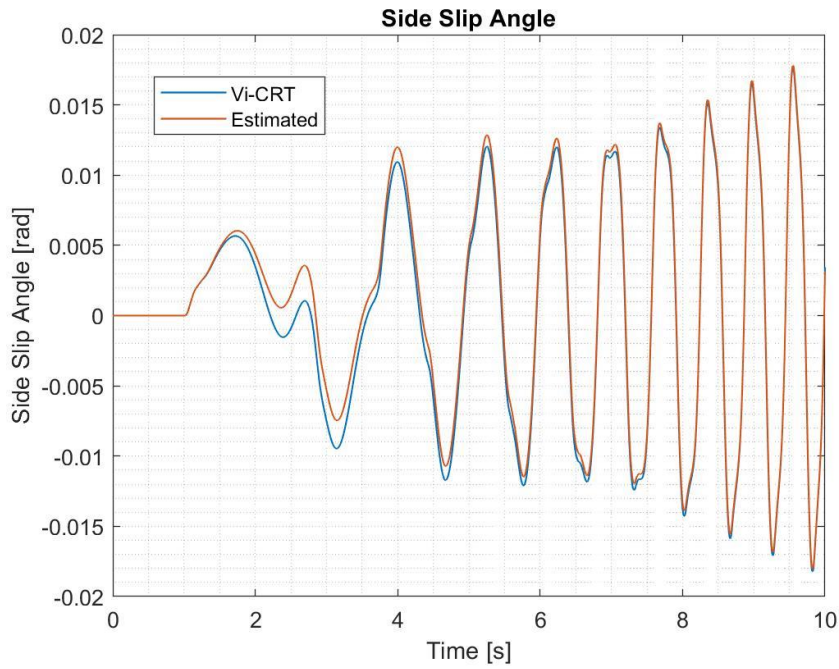


Figure 35: Side Slip Angle estimation vs Vi-CRT output (sine sweep steer) - RMS error = 0.00328 rad

Yaw Control

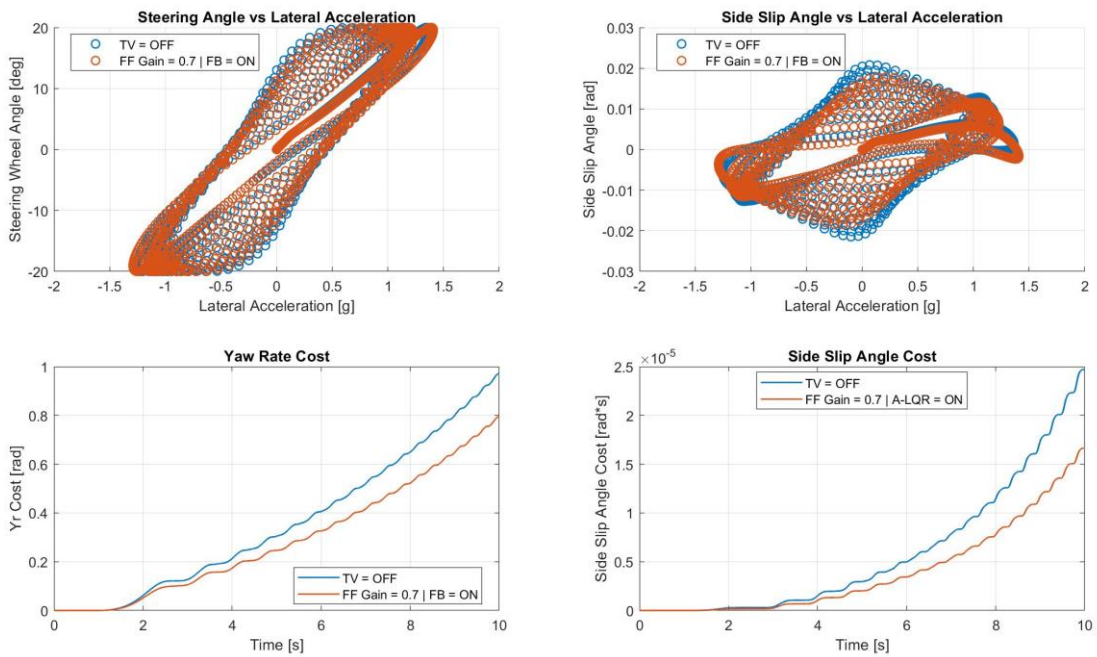


Figure 36: Lateral Characteristics Sine Sweep Steer for vehicle with TV = OFF and TV = ON

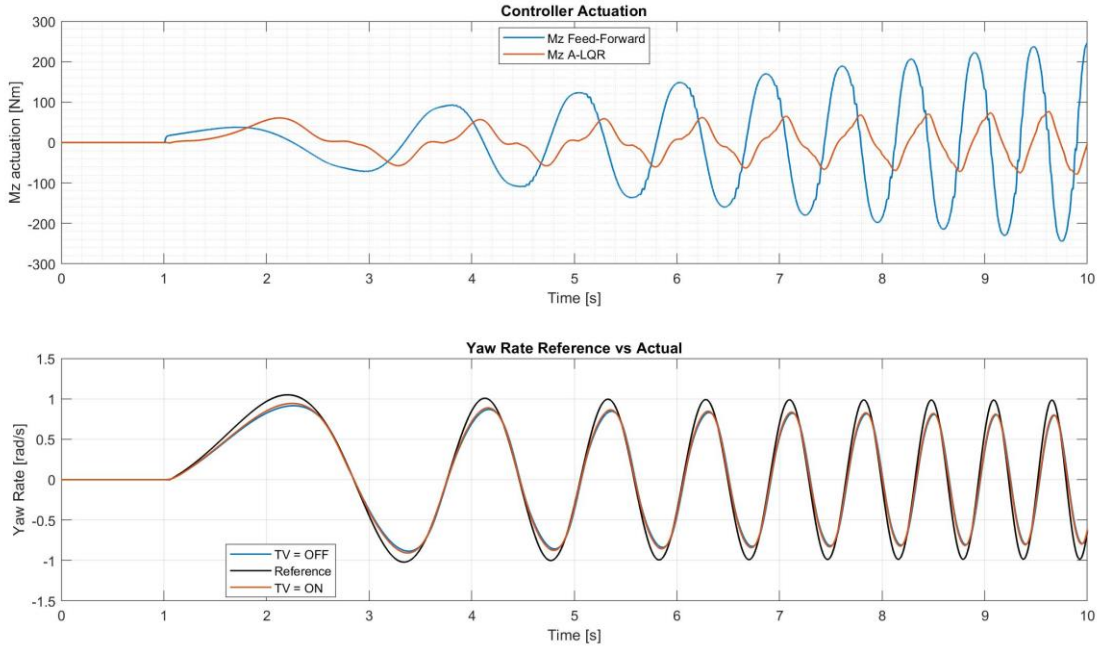


Figure 37: Controller Actuation and Yaw Rates

Side Slip Angle estimation is very good: the contribute of the kinematic-based approach for transients is noticeable, since there is almost perfect tracking along the manoeuvre. The error reduction with time is due to the need of the EKF estimation contribution to converge. RMS error remains very low, 0.00328 rad.

Also, for the Sine Sweep Steer manoeuvre, improvements are noticeable. In the two upper plots, the contribute of the Torque Vectoring can be noted for two reasons: the first is that at the same time, lateral acceleration maximum value increases for the same steering angle input and the hysteresis of that plot decreases, meaning a progressive increasing contribution, increasing steering frequency input. The second reason is that at the same time, also the amplitude of the Side Slip Angle decreases at increasing frequency inputs: this means that the controller is not only able to improve the performances, but also to improve the stability of the vehicle, reducing its overall understeer.

	Yaw Rate Cost	Side Slip Angle Cost
TV = OFF	0.988	2.5e-5
TV = ON	0.801	1.65e-5

Together with that, both Yaw Rate and Side Slip Angle costs are decreased thanks to the torque vectoring intervention.

The Controller Actuation plot shows some interesting Torque Vectoring characteristics: first, the Feed Forward actuation increases with increasing steering frequency input. This was expected from the theoretical bode plot (Figure 18) since the steering frequency range of this maneuver fits exactly in the first part of the bode frequency region in which actuation increases with frequency. Second, Feed Forward and A-LQR have actuation peaks in opposite time instants: when one is at its peak, the other is close to zero, and vice versa. This is interesting because shows how a controller of this type can cooperate in an easy way reducing the overall weaknesses of the controller.

The Yaw Rate plot demonstrates another time that the reactivity of the controlled vehicle is increased: controlled vehicle Yaw Rate peak is always slightly higher, and its derivative is higher, guaranteeing an anticipated peak compared to the uncontrolled vehicle.

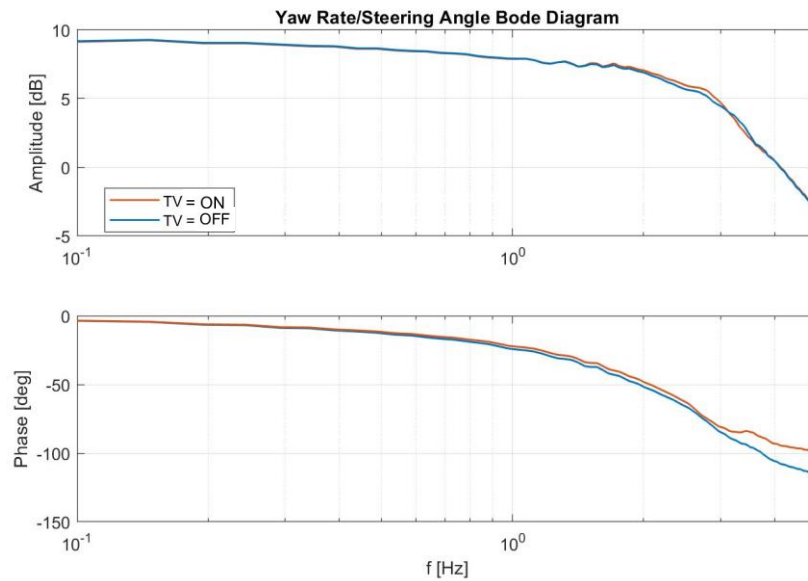


Figure 38: Bode diagram Yaw Rate vs Delta (sine sweep steer) for TV = OFF and TV = ON

Since this manoeuvre involves a steering frequency input increase from start to end, it could be interesting to build a bode diagram starting from logged Yaw Rate and Steering Angle signals. Results are interesting:

- Up to 0.5 Hz steering input, there is no difference between controlled and uncontrolled vehicle.
- From 0.5 Hz to 3 Hz the controlled vehicle is more responsive, being the amplitude of the controlled vehicle is higher.
- Above 3 Hz, the controlled vehicle loses amplitude performances, but anyway it's an unachievable region of steering input frequency.
- Phase margin is always reduced for the controlled vehicle.

Torque Allocation

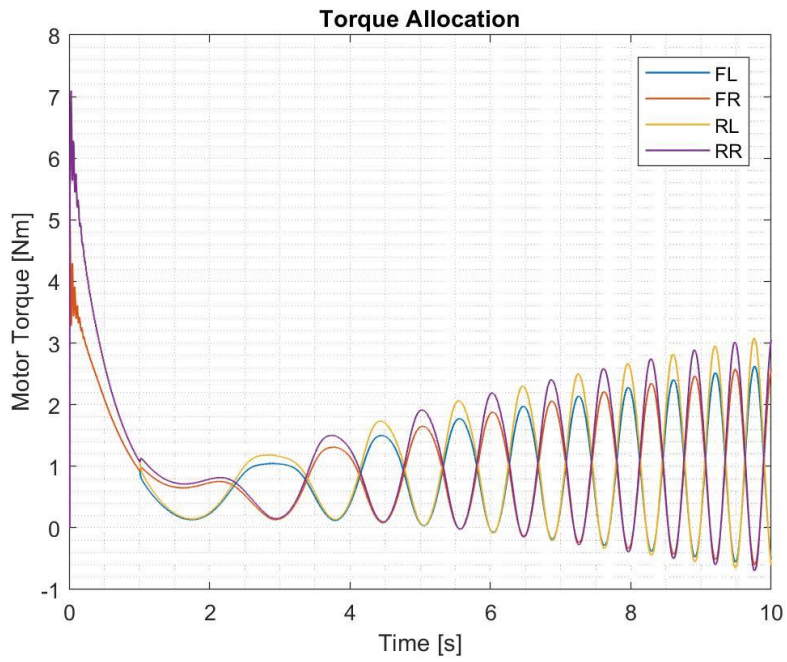


Figure 39: Torque Allocation (Sine sweep steer)

Allocation is very good, no high frequency oscillations occur. The algorithm recognized the necessity of having internal wheel negative torque and also the switch from positive to negative torque is performed smoothly.

4.4. Max Performance Events

Then, since the controller will be introduced in the complete control system of a vehicle competing in FSAE event, it must be tested on the event in which the lateral dynamics is predominant: Skidpad.

The Skidpad track consists of two pairs of concentric circles in a figure of eight pattern. The centres of the two circles are 18.25 meters apart, the track is 3 meters wide, the inner circle has a diameter of 15.25 meters. The vehicle must enter the track from a perpendicular entry line, must travel two times the right circle and two times the left circle and the lap time is considered the average time of the two second laps per each side.

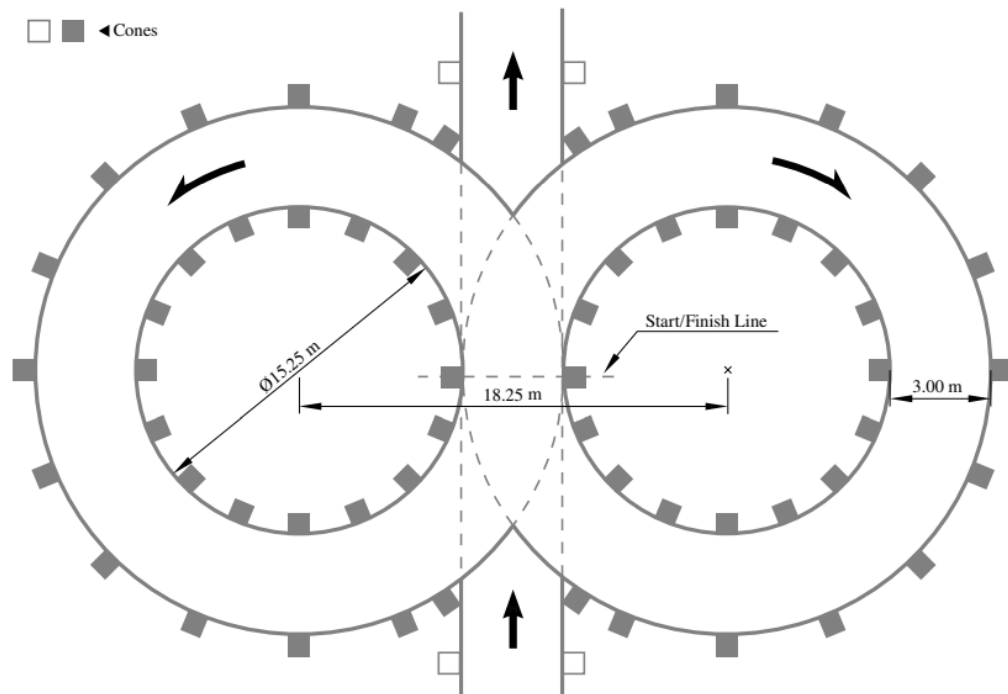


Figure 40: Skidpad Track Layout

On Vi-CRT the Skidpad Track is given by Vi-Grade as one of the layouts in the Vi-Grade Virtual Formula competition starter pack. It is a Max Performance Event that requires as inputs:

- Skidpad entry Speed = 10 m/s
- Longitudinal PF: 0.75
- Lateral PF: 1.2
- Braking PF: 1.2
- Lateral deviation from centre line: 0.75 m

All PF and lateral deviation from centre line have been decided after an iterative process of trial and error to match the vehicle behaviour of Squadra Corse PoliTo Skidpad at FSATA 2022. In particular, the Longitudinal PF is so small compared to other two, otherwise the driver model would enter the Skidpad layout at full throttle: this situation is highly unstable for the tight Skidpad corner and clearly not a realistic situation.

4.4.1. State Estimation

For what concerns State Estimation, in this case, all other important vehicle states for vehicle lateral dynamics are shown to demonstrate the goodness of estimation, being Skidpad a more challenging and realistic manoeuvre compared to the previous.

Vehicle Side Slip Angle

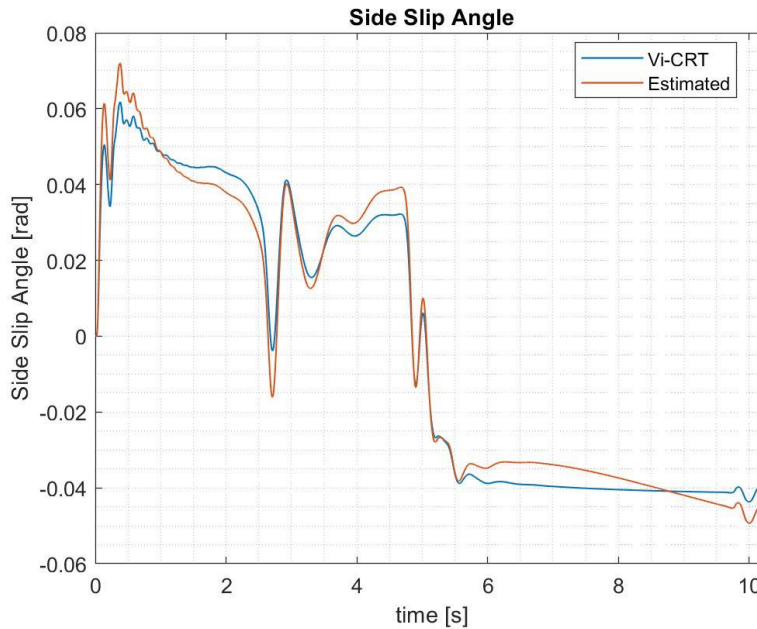


Figure 41: Side Slip Angle comparison

Figure 33 shows the comparison between estimated and Vi-CarRealTime side slip angles, resulting in a good correlation, especially in transient manoeuvres. During steady state manoeuvres, little divergence occurs, probably due to the instability of the kinematic-based approach.

Tire Slip Angle

The tire slip angle is a similar concept compared to the vehicle side slip angle but translated to the tire reference frame. The slip angle is, by definition, the angle

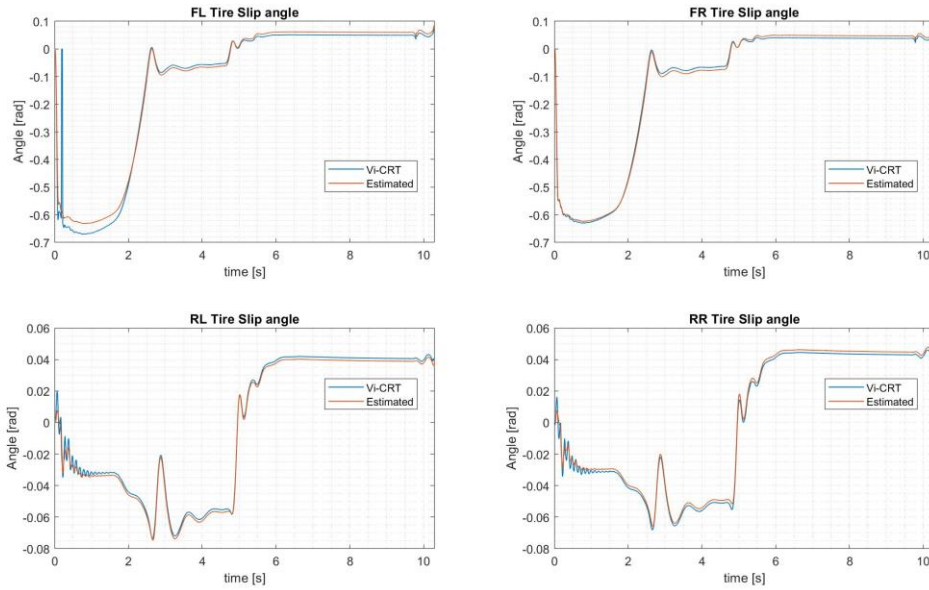


Figure 42: Tire Slip Angle comparison

The precision of the estimation is good, both in transient and steady state parts of the Skidpad.

Tire Normal Force

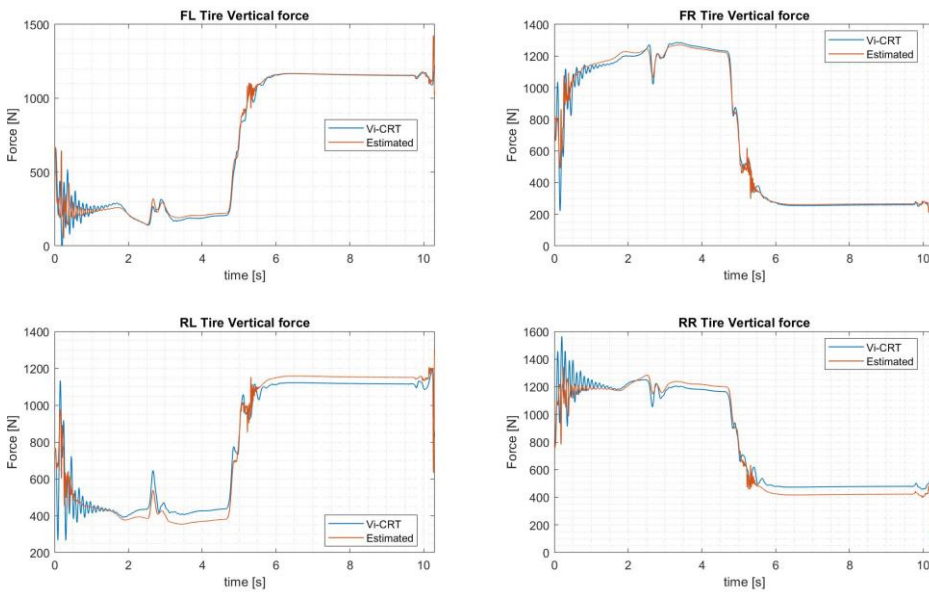


Figure 43: Normal Force comparison

Figure 43 shows the comparison between Vi-CRT output and estimated normal forces. The estimation is good, with correct trends and small relative errors, especially at high vertical load.

Tire Longitudinal Force

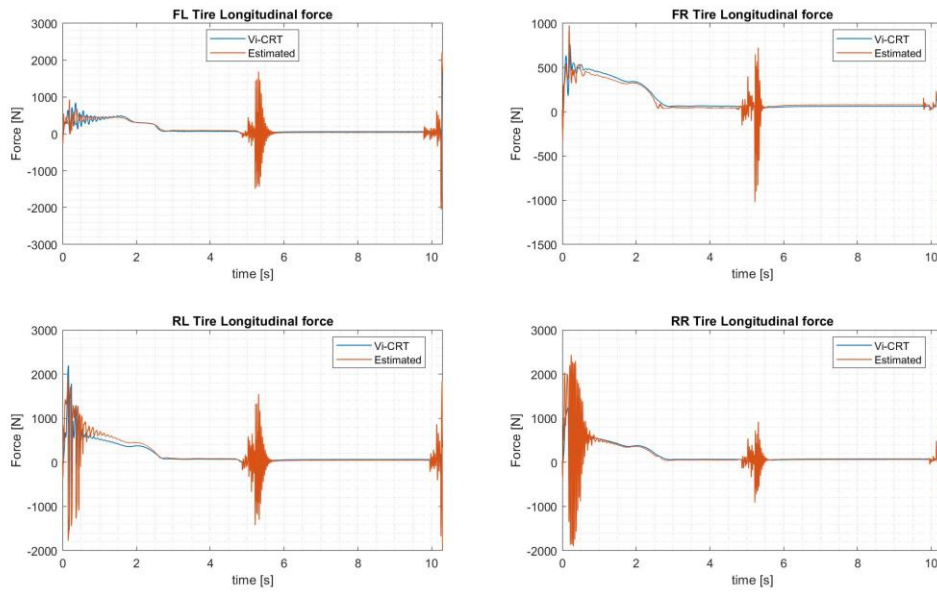


Figure 44: Tire Longitudinal Force comparison

The estimation trend is correct, the steady state tracking is quite good. Oscillation amplitudes during transient manoeuvres are a bit too high, probably due to slip oscillating trend, too.

Tire Lateral Force

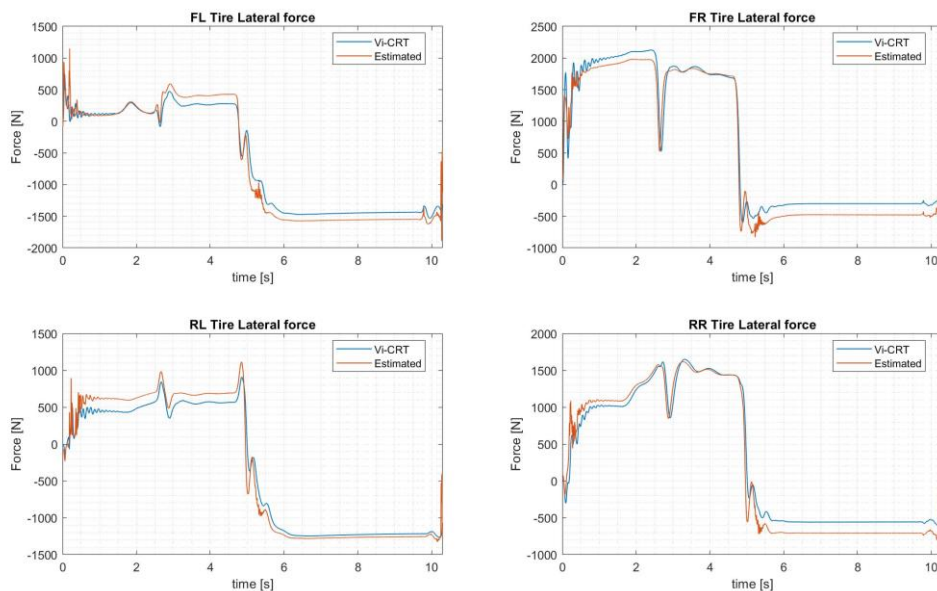


Figure 45: Tire Lateral Forces comparison

The comparison between Vi-CRT output and estimated forces is good, especially for the more loaded couple of tires (the outer ones).

4.4.2. Yaw Control

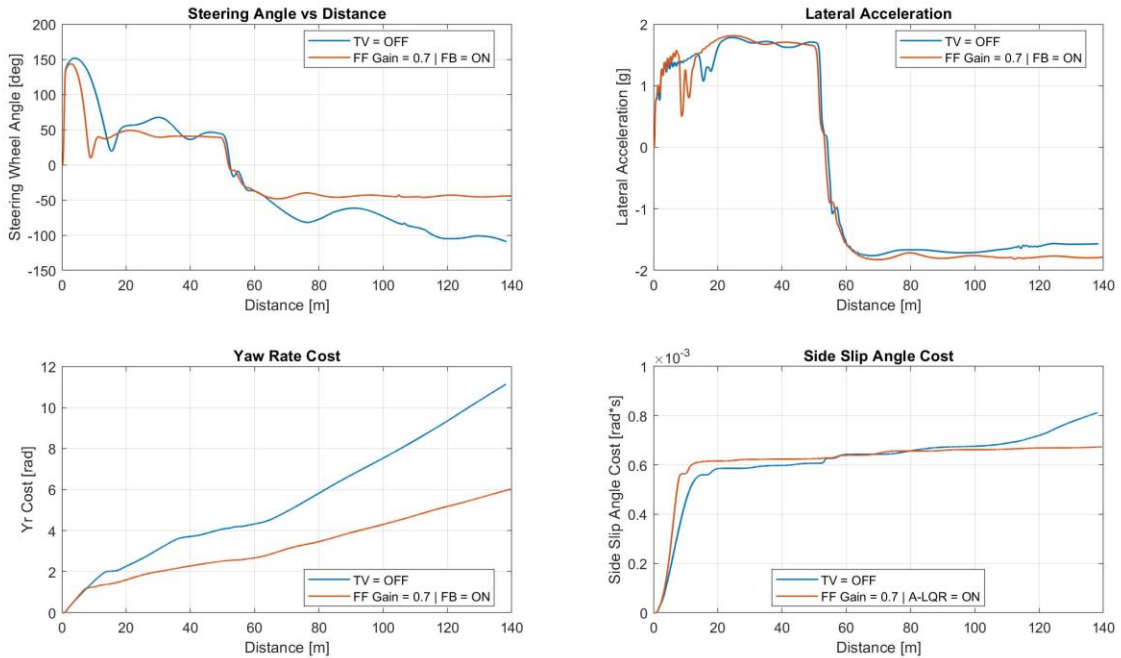


Figure 46: Skidpad Lateral Characteristics for vehicle with TV = OFF and TV = ON

Also, for a real closed loop manoeuvre, with a driver model trying to guarantee maximum performance in a highly demanding couple of corners, the Torque Vectoring improvements are easily noticeable. First, the steering angle demand from driver is always lower and way smoother. Second, the lateral acceleration is higher as average absolute value, in particular, for the second part of the stint. Third, both costs are kept lower as for all other manoeuvres.

	Yaw Rate Cost [rad]	Side Slip Angle Cost [rads]	Lap-time [s]
TV = OFF	11.07	0.00811	9.60
TV = ON	6.01	0.00659	9.02

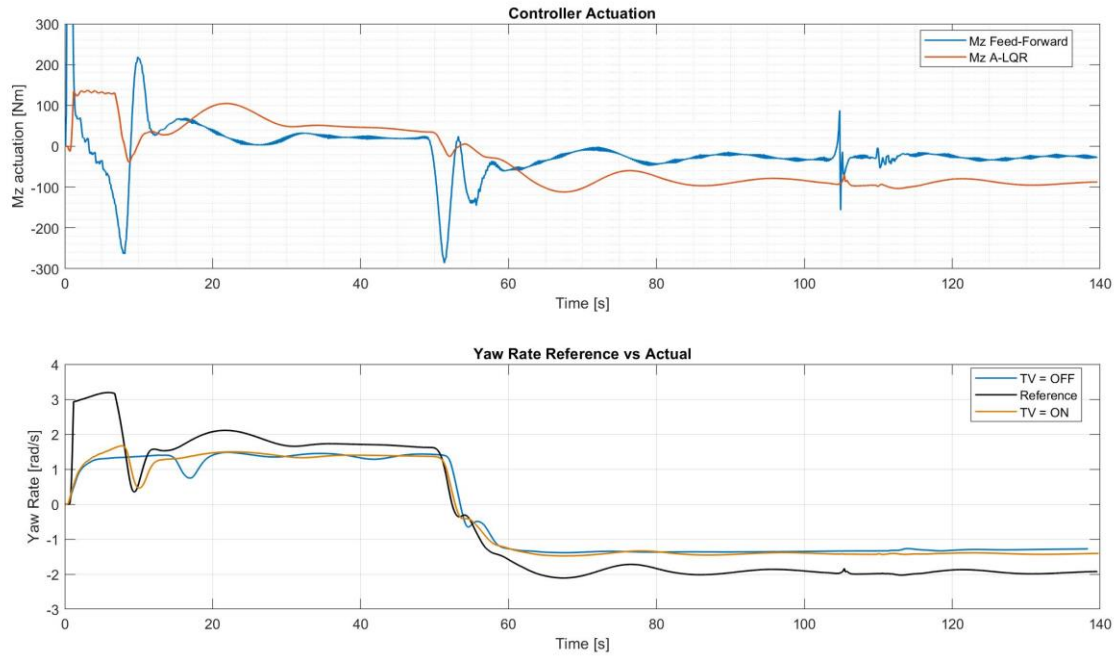


Figure 47: Controller Actuation and Yaw Rates

Also, for a real manoeuvre like the Skidpad, every trend noticed in standard manoeuvres is respected: actuations are always giving maximum contributions in different moments, with Feed Forward carrying the transients and A-LQR the steady state instants. Yaw Rate of the controlled vehicle is smoother and generally higher in absolute value during steady state and anticipated during transients.

4.4.3. Motor Torque Allocation

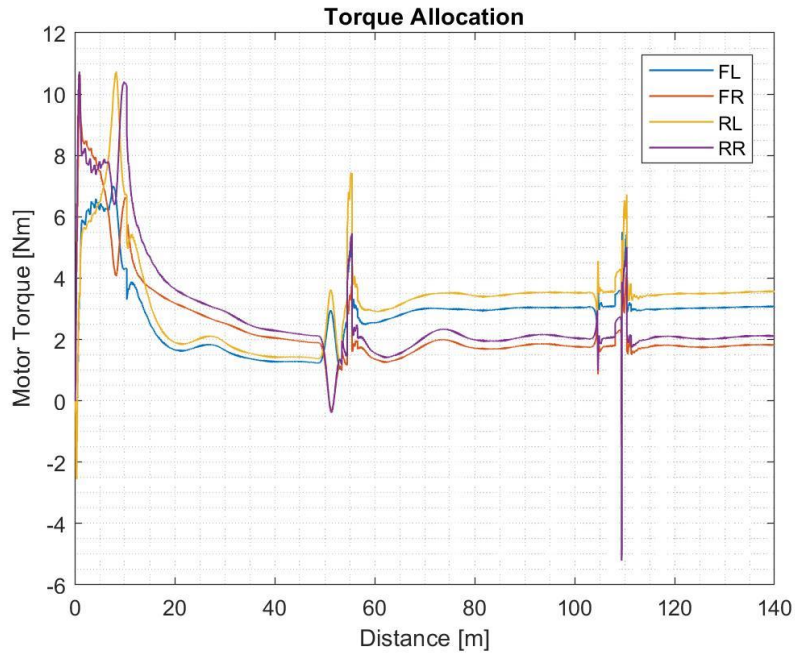


Figure 48: Torque Allocation (Skidpad)

Allocation trend is good, no discontinuities are obtained. Two torque oscillation regions can be individuated, one during change of direction, the other to correct a small oversteering beginning.

5. Experimental Validation

The last section of this thesis has the target of explaining the experimental work done regarding this project: Yaw Control ECU deployment and Sideslip Angle estimator validation.

The vehicle, during testing phase, is always equipped with:

- Ellipse-N IMU (Single Antenna RTK GNSS) for precise acquisition of longitudinal acceleration, lateral acceleration, yaw rate and vehicle speed.
- High-precision potentiometer for steering wheel angle acquisition.
- Motor rotational speed sensors.
- Motor current sensors, for direct torque estimation.
- Two high-precision potentiometers for throttle pedal position sensing, with sensor's redundancy.
- Load cell for brake pedal force.
- Two pressure sensors for brake system pressure acquisition.
- dSpace MicroAutobox II.

5.1. Hardware Deployment

The first target of the experimental validation of the project is the Hardware deployment of Yaw Control and State Estimator. This means that the Simulink-implemented logics must be installed into the vehicle ECU through code generation.

As said above, the vehicle ECU is a dSpace MicroAutobox II 1401/1511 equipped with IBM PPC 750GL processor running at 900 MHz, 16 Mb memory, 16 Mb nonvolatile flash memory containing data recorder.

Since all the logics are developed using Matlab/Simulink, also the code generation is done exploiting this software. In fact, Matlab offers together with dSpace, dedicated tools for can communication (both Tx and Rx) and code generation, just requiring as input the target dSpace ECU. Moreover, CAN .dbc files are needed to be imported into Simulink before code generation, for proper CAN communication. Once all the parameters are set correctly (CAN communication subsystems, target ECU selected), the C code can be generated autonomously. Within all the list of generated files, two of them are of our particular interest:

- .ppc file contains the C code that will be run in real time.
- .sdf file contains the so-called variable description and it's fundamental for the code graphic user interface: every parameter, signal, constant can be monitored real-time using dSpace controldesk Software.

Such software is fundamental to flash the generated code into the ECU and then monitoring that everything is running as expected, through real time data analysis. This is possible because all sensors are cabled into four different CAN Networks

converging into the ECU. The ECU reads inputs in real time and its main target is to require a certain amount of desired torque for each motor.

With this target, the Yaw Control and the SideSlip Angle estimator

- Have been implemented in the complete vehicle control system.
- Have been undergone code generation, without any error or warning.
- Have been flashed into the vehicle ECU without any fault.

Moreover

- Sideslip Angle estimator has been tested real time, giving satisfying results, better explained in the next section.
- Yaw Control has not run real time yet, since the dedicate test session has yet to come.

5.2. Sideslip Angle Estimation Validation

Being the estimation of the Sideslip Angle fundamental for the correct working of the Yaw Control, the testing phase of this subsystem has the priority.

In order to validate an estimator, the state of interest must be, somehow, measured.

For what concerns Sideslip Angle, one way to measure it consists of exploiting optical sensors able to measure longitudinal and lateral velocities, separately and with high accuracies. These two high-precision measurements give the possibility of computing Sideslip Angle instead of estimating it.

Together with all the set of sensors that the vehicle brings along all the tests, for this dedicated session, SC22evo was equipped with a Kistler Ground Speed Sensor (GSS), too.

The considered sensor is the Kistler Correvit SF-Motion, with the following characteristics:

- Reduced signal noise for speed and sideslip angle signals
- Low signal delay of 6 ms
- Possibility to be installed everywhere on the car, with the constraint of being capable to see the road perpendicular to it.
- High-precision measurement of distance, longitudinal and lateral velocities, accelerations, angular rates, sideslip angle, pitch and roll angle.

For this application, the sensor has been decided to be installed at the rear end of the vehicle, slightly behind the rear track centre, through the production of a simple and light-weight aluminium bracket.

Together with the sensor installation, also the integration into one CAN Network has been performed. The .dbc file has been inserted into the Simulink for code generation, giving the vehicle ECU the possibility to correctly read all signals coming from the Correvit SF-Motion. Data are logged through the USB-dedicated ECU output and the data analysis has been performed offline.



Figure 49: Installation of Kistler Correvit SF-Motion

All necessary signals to be logged to perform Sideslip Angle estimation and its validation are the following:

- Longitudinal, Lateral accelerations [g]
- Vehicle velocity [m/s]
- Yaw Rate [rad/s]
- Steering wheel angle [rad]
- Correvit SF-Motion reference measured Sideslip Angle [rad]

First, the sensor must be calibrated, acquiring at least 500 m of straight motion. Then simple low-speed manoeuvres are suggested to be performed, for fine-calibration. Finally, high performance tests can be performed. All the test session has been performed at Cerrina Racetrack, the team standard test track. The considered test involves standard driving at medium-high vehicle performance, as if the vehicle is racing at the Endurance event.

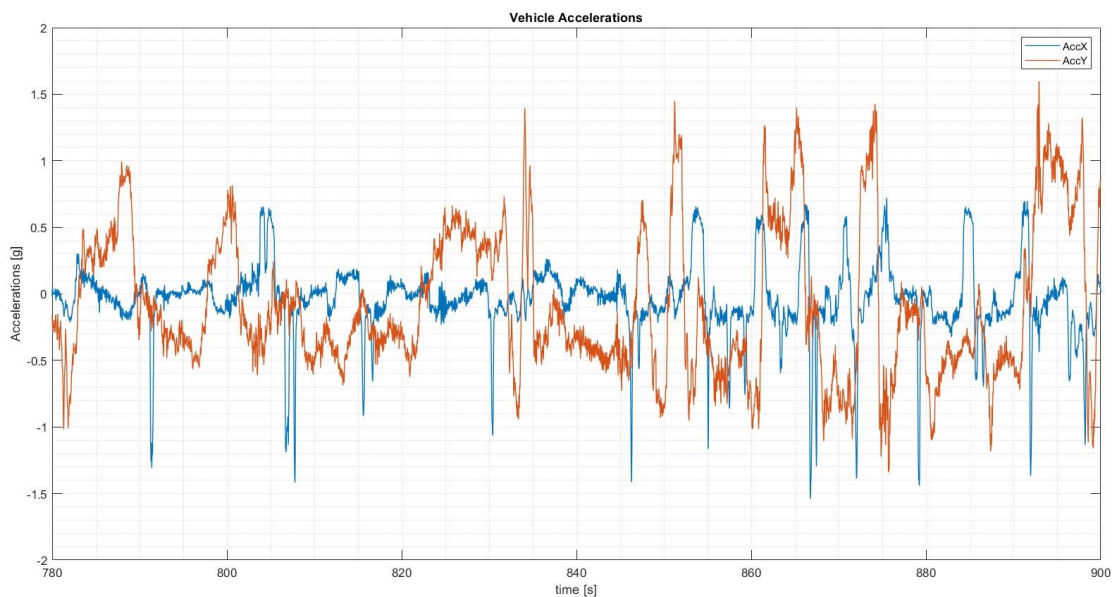


Figure 50: Longitudinal and lateral accelerations during state estimation validation tests.

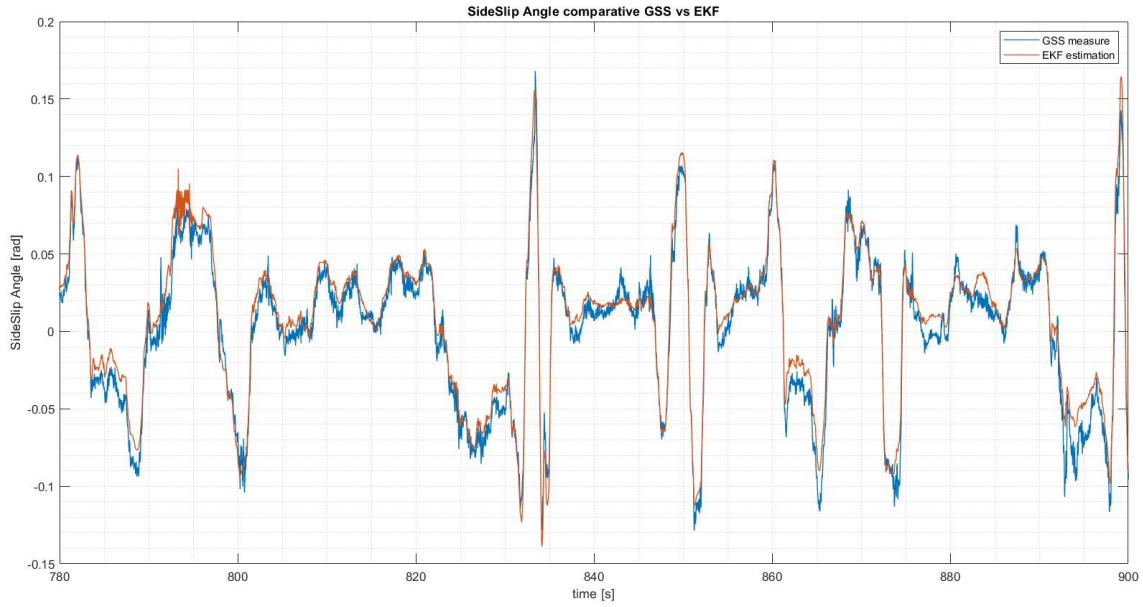


Figure 51: Measured Sideslip Angle vs Estimated Sideslip Angle

Results are satisfying: The estimated sideslip angle always matches measured sideslip angle trends. Peaks are well aligned, and transient dynamics is well modelled.

	RMSE [rad]	GoF (Matlab Function)
Est. vs Meas. Sideslip Angle	0.0172	0.000294

Numerical results confirm what can be seen from figure 51: root mean square error remains below 1 deg, and GoF (goodness of fit) stays very low. This parameter, as Matlab Guide says, demonstrates a good data fitting when it approaches the zero.

For our application, results are good. Since for our use case Sideslip angle is not used of precise trajectory control, but only for stability control, the achieved precision is sufficient. From now on, the Sideslip Angle estimator will be installed in the vehicle ECU as a validated software component, and it will feed the Yaw Control with a sideslip angle that will be considered fully reliable.

Being the estimator model-based and not data driven, it will always be fully reliable, just adjusting the model parameters that will change while the vehicle will upgrade during the seasons.

6. Conclusions and future works

This work aimed to propose a method to implement a Yaw Controller for the application on Electric Vehicles. To develop a proper controller, it is necessary to estimate or measure several vehicle's states. The estimation of those states, starting from the Side Slip Angle estimation, going in a cascade way to contact patch forces estimation, has shown good results. Due to this reason, a model-based controller has been decided to be implemented, combining the state tracking of a LQR together with the reactivity of a feed-forward action. Such controller, together with the Side Slip Angle estimator, has been tested and fine-tuned in MiL using Vi-CarRealTime and Matlab/Simulink co-simulation environment.

The controlled vehicle has shown good results, with improved overall stability and performances. In order to quantify the improvements brought by the controller in all the different studied manoeuvres, some KPIs have been properly selected. The comparison has always been done on the same vehicle, with fixed parameters, just introducing the tuned controller. Improvements are noticeable in every standard manoeuvre and on a real FSAE track, too.

Future developments

Future possible improvements regarding the implemented Yaw Controller on its own are difficult to identify, since the solution has been pushed at its limits. Higher time on the project could be spent on the racetrack, with the goal of validating Yaw Controller, too. Together with that, an intense test session aimed to the real-world fine-tuning of the controller must be done, to push the real vehicle at its limits, too. It could be useful, if needed, to tune the controller according to drivers' needs, having different tunings for different drivers. Finally, during Yaw Controller dedicated tests, an optical sensor can be mounted to measure Side Slip Angle in low, medium and high intensity lateral dynamics tests, to validate the state estimator.

References

- Borase, M. S. (2020). A review of PID control, tuning methods and applications. *International Journal of Dynamics and Control*.
- Chindamo, B. G. (2018). On the Vehicle Sideslip Angle Estimation:. *Applied Sciences*.
- Genta, G., & Morello, L. (2020). *The Automotive Chassis Vol.1*.
- Giancarlo Genta, L. M. (2009). *The Automotive Chassis Vol.2*.
- Goggia, S. D. (2015). Integral Sliding Mode for the Torque-Vectoring Control of Fully Electric Vehicles: Theoretical Design and Experimental Assessment. *IEEE TRANSACTIONS ON VEHICULAR TECHNOLOGY*.
- Manca, R., Molina, L. M., Hegde, S., Tonoli, A., & Amati, N. (2023). *Optimal torque-vectoring control strategy for energy efficiency and vehicle dynamics improvement of battery electric vehicles with multiple motors*.
- Mazzilli V., D. P. (2021, January 26). Integrated chassis control: Classification, analysis and future trends. *Annual Reviews in Control*.
- Pacejka, H. B. (2002). *Tyre and Vehicle Dynamics*.
- Parra, T. G. (2021). On Nonlinear Model Predictive Control for Energy-Efficient Torque Vectoring. *Transaction On Vehicular Technology*.
- Parra, Z. P. (2018). Intelligent Torque Vectoring Approach for Electric Vehicles with Per-Wheel Motors.
- Rajamani, R. (2009). *Development and Experimental Evaluation of a Slip Angle Estimator for Vehicle Stability Control*.
- Tramacere, T. A. (2022). Adaptive LQR Control for a Rear-Wheel Steering Battery Electric Vehicle. *Vehicle Power and Propulsion Conference*.
- Villano, E. (2021). *Cross-combined UKF for vehicle sideslip angle estimation with a modified Dugoff tire model: design and experimental validation*.
- Warth, F. G. (2019). Design of a central feedforward control of torque vectoring and rear-wheel steering to beneficially use tyre information. *Vehicle System Dynamics*.
- Welch, G. (2001). *An Introduction to the Kalman Filter*.
- Welch, G. (2006). *An Introduction to the Kalman Filter*.
- Zanial, R. B. (2017). Yaw Rate and Sideslip Control using PID Controller fro Double Lane Changing.

References

List of Figures

Figure 1: Formula Student Events.....	8
Figure 2: SC05 (Squadra Corse PoliTo 2005 prototype)	10
Figure 3: SC08H (Squadra Corse PoliTo 2010 prototype).....	10
Figure 4: SC12e (Squadra Corse PoliTo 2012 prototype)	10
Figure 5: SC22evo (Squadra Corse PoliTo 2023 prototype).....	12
Figure 6: Downstream ICC Architecture Example (Mazzilli V., 2021)	14
Figure 7: Upstream ICC Architecture (Mazzilli V., 2021).....	15
Figure 8: Simulink high-level model of SC22 Vehicle Control System.....	16
Figure 9: Control System Structure with a focus on what will be developed in this work.....	17
Figure 10: Motors Speed Control	19
Figure 11: Artificial Neural Network (ANN) estimation process high-level schematic (Chindamo, 2018)	22
Figure 12: General layout of an ANN used for Side Slip Angle estimation (Chindamo, 2018).....	23
Figure 13: PID Controller Structure (Borase, 2020).....	25
Figure 14: An example of sliding surface with its boundary layer (Goggia, 2015).....	26
Figure 15: General ISMC structure for Torque Vectoring purpose (Goggia, 2015).	26
Figure 16: General diagram representing Fuzzy Logic approach (Parra Z. P., 2018).	27
Figure 17: An example of FL based Yaw Control.....	28
Figure 18: Simplified block diagram of the NMPC for Yaw Control (Parra T. G., 2021) ...	29
Figure 19: Dual Track Model	31
Figure 20: The Kalman Filter cycle	33
Figure 21: Tire Slip Angle (Genta & Morello, 2020)	34
Figure 22: Tire Slip Angle comparison	35
Figure 23: Tire Longitudinal Force (Magic Formula 6.2)	36
Figure 24: Tire Lateral Force (Magic Formula 6.2).....	36
Figure 25: Bode Diagram of FF(s) varying Desired Inertia Moment.....	39
Figure 26: Bode Diagram of FF(s) varying Vehicle Longitudinal Speed.....	40
Figure 27: Side Slip Angel Estimation vs Vi-CRT output (constant radius cornering) – RMS error = 0.00312 rad	45
Figure 28: Lateral Characteristic Comparison in Constant Radius Cornering for TV OFF and TV ON.....	45
Figure 29: Controller Actuation and Yaw Rate trends for Constant Radius Cornering maneuver	46
Figure 30: Torque Allocation – Constant Radius Cornering.....	47
Figure 31: Side Slip Angle estimation vs Vi-CRT output (ramp steer) – RMS error = 0.00147 rad.....	48
Figure 32: Lateral characteristic comparison in Ramp Steer with TV = OFF and TV = ON.....	48
Figure 33: Controller actuations and Yaw Rates (ramp steer)	49
Figure 34: Torque Allocation (ramp steer).....	50
Figure 35: Side Slip Angle estimation vs Vi-CRT output (sine sweep steer) - RMS error = 0.00328 rad.....	51
Figure 36: Lateral Characteristics Sine Sweep Steer for vehicle with TV = OFF and TV = ON	51
Figure 37: Controller Actuation and Yaw Rates	52

Figure 38: Bode diagram Yaw Rate vs Delta (sine sweep steer) for TV = OFF and TV = ON	53
Figure 39: Torque Allocation (Sine sweep steer)	54
Figure 40: Skidpad Track Layout.....	55
Figure 41: Side Slip Angle comparison.....	56
Figure 42: Tire Slip Angle comparison.....	57
Figure 43: Normal Force comparison.....	57
Figure 44: Tire Longitudinal Force comparison	58
Figure 45: Tire Lateral Forces comparison	58
Figure 46: Skidpad Lateral Characteristics for vehicle with TV = OFF and TV = ON.....	59
Figure 47: Controller Actuation and Yaw Rates	60
Figure 48: Torque Allocation (Skidpad)	61
Figure 49: Installation of Kistler Correxit SF-Motion	64
Figure 50: Longitudinal and lateral accelerations during state estimatoion validation tests.....	64
Figure 51: Measured Sideslip Angle vs Estimated Sideslip Angle.....	65

List of Tables

Table 1: SC22evo prototype main data.....	12
Table 2: Numerical Comparison of State Costs with TV = OFF and TV = ON	46